ADVANCES IN OSCILLOMETRIC BLOOD PRESSURE MEASUREMENT

By

Anand Chandrasekhar

A DISSERTATION

Submitted to
Michigan State University
in partial fulfillment of the requirements
for the degree of

Electrical Engineering – Doctor of Philosophy

ABSTRACT

ADVANCES IN OSCILLOMETRIC BLOOD PRESSURE MEASUREMENT

By

Anand Chandrasekhar

High blood pressure (BP) is a major cardiovascular risk factor that is treatable, yet hypertension awareness and control rates are low. Ubiquitous BP monitoring technology could improve hypertension management, but existing devices require an inflatable cuff and are not compatible with such anytime, anywhere measurement of BP. Oscillometry is the blood pressure (BP) measurement principle of most automatic cuff devices. We extended the oscillometric principle, which is used by most automatic cuff devices, to develop a couple of instruments to measure cuff-less BP using a smartphone-based device and standalone iPhone application. As the user presses her/his finger against the smartphone, the external pressure of the under lying artery is steadily increased while the phone measures the applied pressure and resulting variable amplitude blood volume oscillations. A smartphone application provides visual feedback to guide the amount of pressure applied over time via the finger pressing and computes systolic and diastolic BP from the measurements.

We prospectively tested the smartphone-based device for real-time BP monitoring in human subjects to evaluate usability (n = 30) and accuracy against a standard automatic cuff-based device (n = 32). We likewise tested a finger cuff device, which uses the volume-clamp method of BP detection. About 90% of the users learned the finger actuation required by the smartphone-based device after one or two practice trials. The device yielded bias and precision errors of 3.3 and 8.8 mmHg for systolic BP and -5.6 and 7.7 mmHg for diastolic BP over a 40 to 50 mmHg range of BP. These errors were comparable to the finger cuff device. Cuff-less and calibration-free monitoring of systolic and diastolic BP may be feasible via a smartphone. In addition, we tested the iPhone application. The application yielded bias and precision errors of -4.0 and 11.4 mmHg for systolic BP and -9.4 and 9.7 mmHg for diastolic BP (n = 18). These errors were near the finger cuff device errors. This proof-of-concept study surprisingly indicates that cuff-less and calibration-free BP

monitoring may be feasible with many existing and forthcoming smartphones.

These devices use empirical algorithms, already descried in the literature, to estimate blood pressure. Hence, the next objective was to establish formulas to explain three popular empirical algorithms- the maximum amplitude, derivative, and fixed ratio algorithms. A mathematical model of the oscillogram was developed and analyzed to derive parametric formulas for explaining each algorithm. Exemplary parameter values were obtained by fitting the model to measured oscillograms. The model and formulas were validated by showing that their predictions correspond to measurements. The formula for the maximum amplitude algorithm indicates that it yields a weighted average of systolic and diastolic BP (0.45 and 0.55 weighting) instead of commonly assumed mean BP. The formulas for the derivative algorithm indicate that it can accurately estimate systolic and diastolic BP (<1.5 mmHg error), if oscillogram measurement noise can be obviated. The formulas for the fixed ratio algorithm indicate that it can yield inaccurate BP estimates, because the ratios change substantially (over a 0.5-0.6 range) with arterial compliance and pulse pressure and error in the assumed ratio translates to BP error via large amplification (>40). The established formulas allow for easy and complete interpretation of perhaps the three most popular oscillometric BP estimation algorithms in the literature while providing new insights. The model and formulas may also be of some value towards improving the accuracy of automatic cuff BP measurement devices.

Copyright by ANAND CHANDRASEKHAR 2019 This thesis is dedicated to my parents, sister and Priya.

ACKNOWLEDGEMENTS

I had an unforgettable time with my adviser Prof. Mukkamala, without whom it would have been almost impossible to complete my Ph.D. program. His friendly nature was of immense help during my academic life and his emotional support often helped me get back on the right track when I got lost in research.

Also, I would like to thank all my committee members (Prof. Fathi Salem, Prof. Selin Aviyente and Prof. Seungik Baek) for their valuable inputs during my presentations. In addition, I would like to thank all my colleagues (Mohammad Yavarimanesh, Mingwu Gao, Jiankun Liu, Mohsen Moslehpour and Keerthana Natrajan) for all their constructive criticism on my research.

This will be an incomplete acknowledgment without a mention on my family and friends. They were supportive and backed me in tough times. I extend my sincere thanks to them for their help. Last but not the least, I thank the Almighty for all that have happened in my life.

TABLE OF CONTENTS

LIST OF	FFIGURES	X
1.1 1.2 1.3 1.4	Cardiovascular system and Cardiovascular diseases	1 1 1 2
CHAPT		
2.1 2.2	Introduction	3 4 4
	2.2.1.1 Concept	4 4 6
	2.2.2.1 Usability	68
2.3	Discussion	
2.4	Materials and Methods	
	2.4.1 Study design	
	2.4.2 Device development	
	2.4.2.2 Prototype Hardware	
	2.4.2.3 Software	
	2.4.3 Device testing	
	2.4.3.2 Experimental Measurements and Protocol	3
	2.4.3.3 Data Analaysis	
	2.4.3.4 Statistical analysis	
2.5	Conclusion	.5
CHAPT	ER 3 AN IPHONE APPLICATION FOR BLOOD PRESSURE MONITORING VIA THE OSCILLOMETRIC FINGER PRESSING METHOD 2	26
3.1	Introduction	6
3.2	Results	7
	3.2.1 iPhone Application	7
	3.2.2 Usage	8
	3.2.3 Accuracy	8
3 3	Discussion	0

3.4	Materials and Methods
	3.4.1 Application Development
	3.4.2 Application Testing
	3.4.2.1 Experimental Protocol
	3.4.2.2 Data Analysis
3.5	Conclusion
СНАРТ	ER 4 FORMULAS TO EXPLAIN POPULAR OSCILLOMETRIC BLOOD
	PRESSURE ESTIMATION ALGORITHMS
4.1	Introduction
4.2	The Formulas
	4.2.1 Mathematical Model
	4.2.2 Formula for the maximum amplitude algorithm
	4.2.3 Formulas for the derivative algorithm
	4.2.4 Formulas for the fixed ratio algorithm
4.3	Results
	4.3.1 Mathematical model and parameter estimates
	4.3.2 Formula for the maximum amplitude algorithm
	4.3.3 Formula for the derivative algorithm
	4.3.4 Formulas for the fixed ratio algorithm
4.4	Discussion
4.5	Materials and methods
	4.5.1 Patient Data
	4.5.2 Data analysis
4.6	Conclusion
СНАРТ	ER 5 FUTURE WORK
BIBLIO	GRAPHY

LIST OF FIGURES

Figure 2.1:	From conventional cuff-based blood pressure measurement to cuff-less BP monitoring using a smartphone	5
Figure 2.2:	Smartphone-based device for real-time monitoring of BP via the oscillometric finger-pressing method	7
Figure 2.3:	Device usability results (n = 30 new users)	9
Figure 2.4:	Device accuracy results (n = 32 users)	11
Figure 2.5:	Smartphone-based device hardware	18
Figure 2.6:	Smartphone-based device software	22
Figure 2.7:	Human study design for device testing	24
Figure 3.1:	An iPhone application for cuff-less and calibration-free blood pressure (BP) monitoring via extension of the oscillometric cuff measurement principle	29
Figure 3.2:	Application accuracy results (n = 18 users)	31
Figure 4.1:	Oscillometric blood pressure (BP) measurement principle, which is employed by most automatic cuff devices, and associated algorithms.	37
Figure 4.2:	Previous mathematical model of the oscillogram	40
Figure 4.3:	Extended mathematical model of the oscillogram	41
Figure 4.4:	Model and formula parameter values obtained by fitting the model to measured oscillograms from patients	46
Figure 4.5:	Validation results for the formula for explaining the maximum amplitude algorithm	47
Figure 4.6:	Validation results for the formulas for explaining the derivative algorithm	48
Figure 4.7:	Validation results for the formulas for explaining the fixed ratio algorithm	50
Figure 4.8:	Summary of the established formulas for explaining popular oscillometric BP estimation algorithms	54

Figure 5.1:	Future $\mbox{version}(1)$ of the smartphone based BP monitoring device	 58
Figure 5.2:	Future version (2) of the smartphone based BP monitoring device.	 58

CHAPTER 1

INTRODUCTION

1.1 Cardiovascular system and Cardiovascular diseases

Heart is one of the principal organs of the cardiovascular system and is responsible for pumping oxygenated blood to cells via blood vessels. These blood vessels are called arteries. All diseases related to heart and arteries are called Cardiovascular diseases (CVD). One of the most common types of CVD is called atherosclerosis. Such diseases, if not detected in the early stages, may be life-threatening.

1.2 High Blood Pressure: A risk factor for Cardiovascular diseases

CVDs are one of the leading causes of mortality, and hypertension or High Blood Pressure (BP) is one of the significant risk factors for CVDs (Lewington et al., 2002). Despite that, Hypertension awareness and control rates are lacking in the general population, even though there are many devices to measure BP (Ibrahim & Damasceno, 2012). If hypertension awareness rate (percentage of population who are aware that that have hypertension) is around 45% is developing countries and maybe around 55% in developed countries(Ibrahim & Damasceno, 2012). Also, the hypertension control rate (percentage of population who have hypertension under control) is abysmally low. These rates are alarmingly low mainly due to limitations of the devices which we use for measuring blood pressure.

1.3 BP monitoring devices

There are many devices available in the market that can be used to measure blood pressure.

- 1. Few devices BP monitoring devices/methods used in hospital are listed here.
 - Catheterization.

- Auscultation.
- Volume Clamping (Imholz et al., 1998).
- Tonometry.
- 2. Few devices BP monitoring devices/methods used in home/offices are listed here.
 - Oscillometry based BP measurement.
 - Pulse Transit Time based BP measurement.

The study objective of this research is to

- 1. To establish truly cuff-less and calibration free BP measurement devices that can be readily used by many.
- 2. To employ mathematical modeling of oscillometry towards improving algorithm to estimate BP accurately.

1.4 Organization

This thesis will present a couple of new devices to measure blood pressure via a smartphone. Chapter 2 discusses a smartphone based device for blood pressure monitoring via the oscillometric finger pressing method. Chapter 3 reports an iPhone application for blood pressure monitoring via the oscillometric finger pressing method. Chapter 4 introduces a mathematical model of oscillometry to explain the many popular empirical algorithms used in BP estimation. At the end, chapter 5 discuss the future research.

CHAPTER 2

SMARTPHONE-BASED BLOOD PRESSURE MONITORING VIA THE OSCILLOMETRIC FINGER-PRESSING METHOD

2.1 Introduction

High blood pressure (BP) is a major risk factor for strokes and heart disease (Lewington et al., 2002) that is treatable with lifestyle changes and medication (Psaty et al., 1998). However, hypertension awareness and control rates are low (Ibrahim & Damasceno, 2012). Only 55% of hypertensives in developed nations and 45% of hypertensives in developing nations are aware of their condition, and 15% of hypertensives have their BP under control. Ubiquitous BP monitoring technology could improve hypertension awareness by providing serial measurements from the mass population during daily life (Pickering et al., 2006) and enhance hypertension control by providing continual feedback to the individual patient (Agarwal et al., 2011). However, existing noninvasive devices require an inflatable cuff and therefore are not feasible for such anytime, anywhere monitoring of BP.

We proposed to extend the oscillometric principle, which is the basis of most automatic cuff-based BP measurement devices (Alpert et al., 2014)(Van Montfrans, 2001), for cuffless BP measurement using a smartphone. In this scenario, the user serves as the actuator (instead of the cuff) by pressing her/his finger against the phone to vary the external pressure of the underlying artery, whereas the phone serves as the sensor (rather than the cuff) to measure the resulting variable-amplitude blood volume variations or oscillations and applied pressure. The phone also provides visual feedback to guide the amount of finger pressure applied over time and computes BP from the measurements.

To investigate the oscillometric finger-pressing method, we developed a smartphone-based device to implement the method in real time. We then prospectively tested the device in human subjects for usability and accuracy against a standard cuff device. We likewise tested a finger cuff

device, which uses the volume-clamp method, to determine BP (Imholz et al., 1998). Our results indicate that smartphone-based BP monitoring is easily performed via finger actuation and can measure BP with accuracy similar to the finger cuff device.

2.2 Results

2.2.1 Concept Prototype, and Usage

2.2.1.1 *Concept*

The smartphone-based device represents an extension of the oscillometric principle for cuff-less BP monitoring. As shown in Fig. 2.1(A), in conventional oscillometry, the cuff serves as an actuator to vary the external pressure of an artery and as a sensor to measure this pressure and the resulting variable-amplitude blood volume oscillations within the artery. BP is then computed from the oscillation amplitudes as a function of the applied pressure (henceforth called the "oscillogram"). As shown in Fig. 2.1(B), for the smartphone-based device, the user serves as the actuator by pressing her/his finger against the phone to steadily increase the external pressure of the underlying artery (transverse palmar arch artery), whereas the phone, embedded with photoplethysmography (PPG) and force transducers, serves as the sensor to measure the blood volume oscillations and applied pressure. PPG is a well-known optical technique in which a tissue sample is illuminated and the changes mainly in light absorption due to the pulsatile blood volume within the tissue are measured (Mukkamala et al., 2015). The phone also provides visual feedback to guide the amount of finger pressure applied over time, as shown in Fig. 2.1(C), and then likewise computes BP from the oscillogram, as shown in Fig. 2.1(D).

2.2.1.2 *Prototype*

Figure 2.2 (A and B) shows the smartphone-based device. The prototype device is a three-dimensional (3D)–printed case affixed to the back of a smartphone. The case houses a PPG sensor on top of a force transducer to measure the blood volume oscillations and applied finger pressure,

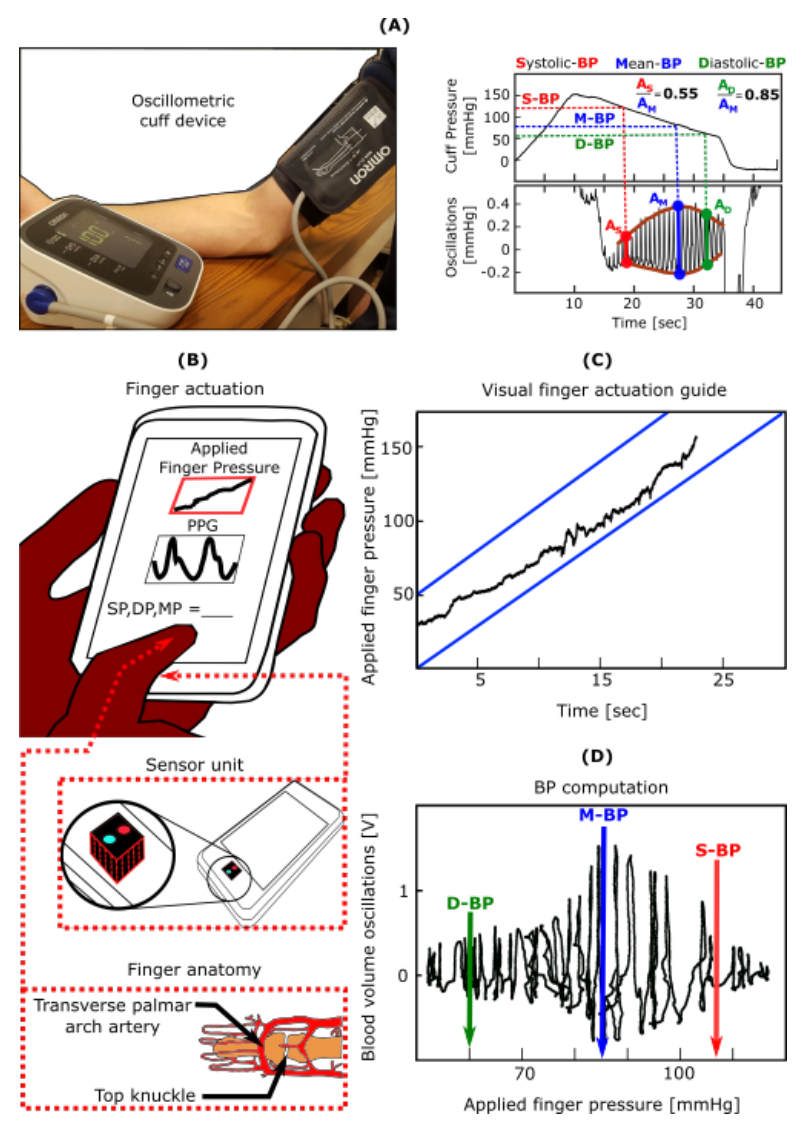


Figure 2.1: From conventional cuff-based blood pressure measurement to cuff-less BP monitoring using a smartphone. (A) Image of a conventional cuff-based oscillometric device and diagram of representative blood pressure (BP) measurement. (B) Schematic diagrams of the proposed oscillometric finger-pressing method for cuff-less BP monitoring using a smartphone, in which the user serves as the actuator instead of the cuff, to vary the external pressure of the transverse palmar arch artery by finger pressing, whereas the phone serves as the sensor to measure blood volume oscillations and applied pressure similar to a cuff, provides a visual display of the applied finger pressure over time to guide the actuation (C), and computes BP similar to a cuff (D). Image of finger anatomy adapted from (Strauch & de Moura, 1990).

as well as circuitry to acquire and transmit the measurements to the smartphone (Fig. 2.2(A)). The smartphone runs an application to visually guide the finger actuation and compute systolic, diastolic, and mean BP at the brachial artery from the finger blood volume oscillation and finger pressure measurements (Fig. 2.2(B)).

2.2.1.3 *Usage*

As shown in Fig. 2.2 (C to E), a user interacts with the device to measure BP in three steps. First, the user places her/his index finger on the sensor so that the base of the finger nail is aligned with "line 1" on the back of the phone and that the long axis of the finger is centered on "line 2" (Fig. 2.2(C)). In this way, measurement from the transverse palmar arch artery may be targeted (Fig. 2.1(B)). The user also rests a portion of the same finger below the top knuckle on the case surface to ensure force application in the normal direction relative to this surface (Fig. 2.2(D)). Second, the user holds the device at the same height as the heart to eliminate hydrostatic effects while viewing the smartphone screen (Fig. 2.2(E)). Third, the user presses her/his finger against the sensor to steadily increase the external pressure of the artery, such that the external pressure application acts similar to a cuff to press the artery against the supporting bone (Fig. 2.1(C)). The user maintains the applied pressure within the target blue lines: Pressure is displayed as it evolves in real time via the smartphone application (Fig. 2.2(B)). After sufficient finger pressure is achieved, the measurement automatically terminates, and the BP measurements are displayed. If the applied pressure falls outside the target lines or the oscillogram quality is deemed inadequate due to a measurement or computation failure, then the device asks the user to try again.

2.2.2 Device Testing

2.2.2.1 *Usability*

To test device usability, 30 new users (age, 39 ± 10 years; height, 168 ± 8 cm; weight, 79 ± 18 kg; 67% females) participated. Each user was allowed practice trials to learn the finger actuation procedure. Figure 2.3(A) shows a histogram of the number of practice trials required for each user

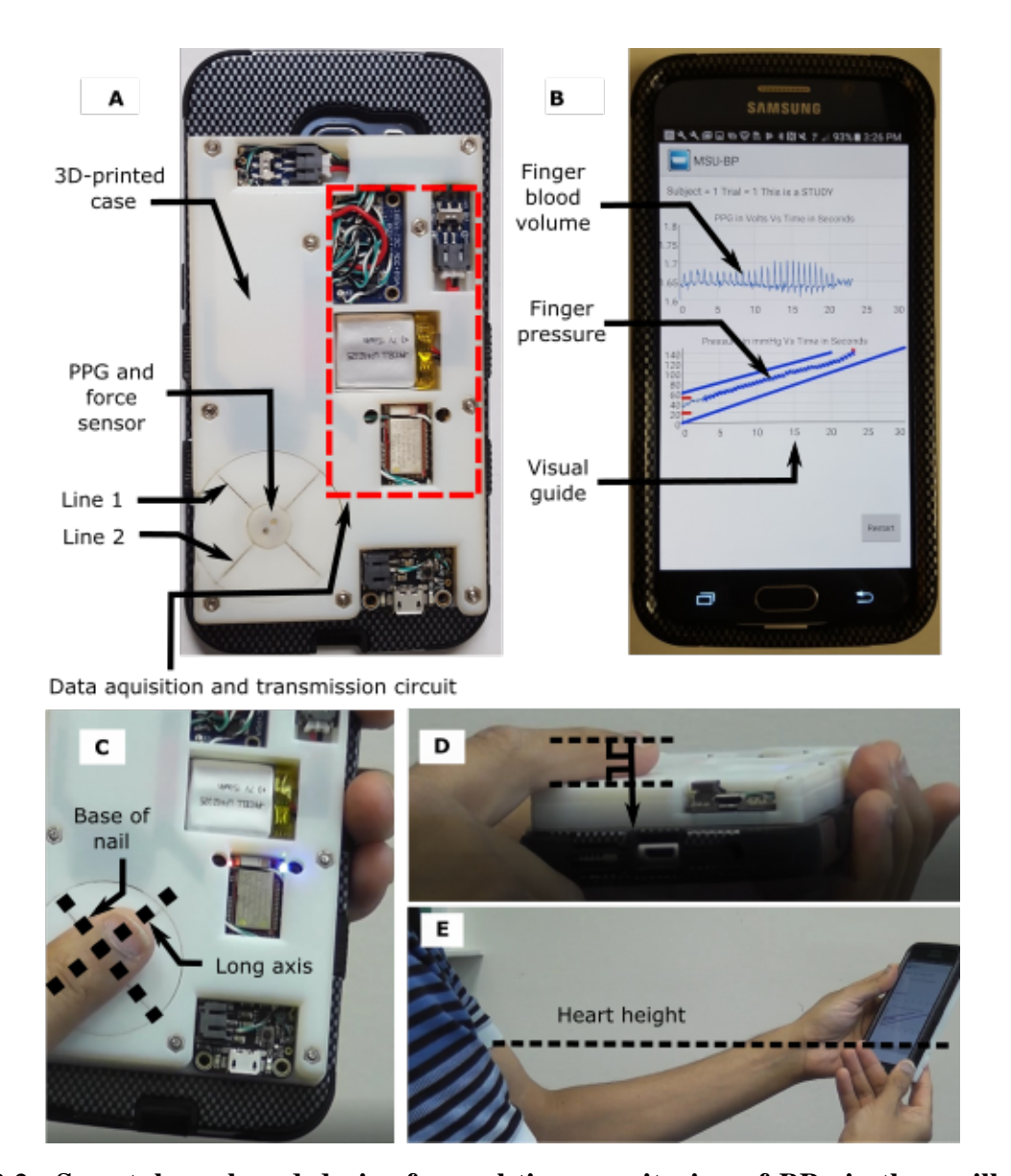


Figure 2.2: Smartphone-based device for real-time monitoring of BP via the oscillometric finger-pressing method. (A) Photograph of the smartphone-based device. A three-dimensional (3D)–printed case was affixed to the back of a smartphone. The case includes visual line indicators to guide finger placement and houses photoplethysmography (PPG) and force sensors along with other circuitry to acquire and transmit the finger blood volume oscillation and applied finger pressure measurements to the phone. (B) Photograph of an application running on the phone to provide visual guidance for the finger actuation and display the finger measurements. Photographs illustrating that a user places her/his finger on the sensor according to the line indicators (C), rests the same finger on the surface of the case to apply force in the normal direction with respect to the case (D), and holds the device at the same height as the heart (E).

to correctly execute the finger actuation, maintaining the applied finger pressure within the target blue lines on the smartphone application. About 90% of the users learned the finger actuation after one or two trials. After learning the finger actuation, each user then performed the finger actuation two to four times with the aim of obtaining a pair of close or three BP measurements. Figure 2.3(B) shows a histogram of the output of the device (BP measurement or "try again" message) overall measurements. About 60% of the measurements were successful. Figure 2.3(C) shows a histogram of the number of try again messages outputted by the device for each user. The device did not output a try again for about 50% of the users and yielded multiple BP measurements for about 80% of the users. However, the device did not output any BP measurements for 2 of the 30 users. Figure 2.3(D) shows a histogram of the reasons for the try again messages. Almost 60% of the try again messages were due to a computation failure. The remaining try again messages were almost exclusively due to a measurement failure. Actuation failure was rare. Computation failure is relatively easy to correct and was the reason that the device did not produce any BP measurement in one of the users.

2.2.2.2 Accuracy

To test device accuracy, the same 30 new users and 5 additional experienced users (age, 33 ± 8 years; height, 173 ± 4 cm; weight, 72 ± 5 kg; 0% females) participated. The latter five users also obtained multiple BP measurements but held the device well below the heart to raise their BP. Device measurements during this hydrostatic challenge may be thought of as BP from a brachial artery situated beneath the heart. The BP measurements from the device were averaged when more than one measurement was available and were assessed against the average of two measurements from a standard oscillometric arm cuff device. Figure 2.4 (A to D) shows the correlation and Bland-Altman plots for the systolic and diastolic BP measurements from the 32 users for which the smartphone-based device yielded BP measurements, and the reference device produced valid BP values. The smartphone-based device yielded bias errors (μ) and precision errors (σ) of 3.3 and 8.8 mmHg for systolic BP and -5.6 and 7.7 mmHg for diastolic BP over a 40 to 50 mmHg

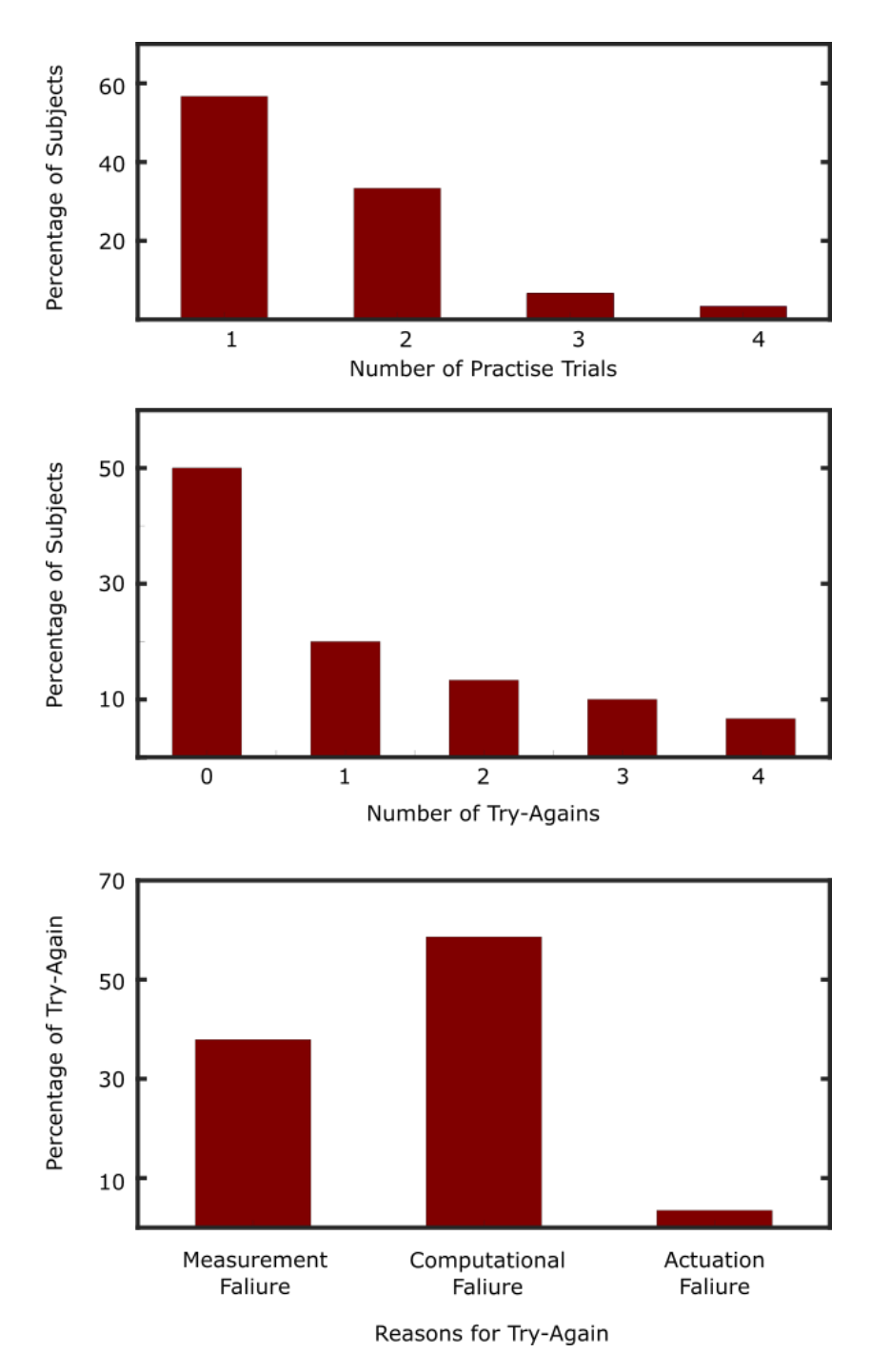


Figure 2.3: **Device usability results** (**n** = **30 new users**). Histograms of the (A) number of practice trials needed to learn the requisite finger actuation for all users; (B) percentage of BP measurements versus try again messages outputted by the device over all users; (C) number of try again messages per user; and (D) reasons for the try again messages.

range of BP. Figure 2.4 (E to H) shows corresponding plots for a finger cuff device, which uses the volume clamp method and likewise computes brachial BP from finger measurements. The smartphone-based device showed BP measurement accuracy similar to the finger cuff device with respect to the standard arm cuff device. However, unlike the smartphone-based device, the finger cuff device always yielded BP measurements.

2.3 Discussion

We proposed the oscillometric finger pressing method for cuff-less BP monitoring using a smartphone. This method may be implemented with a PPG sensor, which measures pulsatile blood volume (Mukkamala et al., 2015), and a force sensor. These sensors are already integrated in many smartphones (Martonik, 2014), although some customization of the sensor architecture is necessary to enable BP measurements. Because the user serves as the actuator to apply external pressure to the transverse palmer arch artery in her/his index finger, the requisite hardware that performs BP measurements is miniaturized and greatly simplified compared to possible alternative methods that would automatically vary the external pressure. Therefore, it may be relatively easy to incorporate the components required by the oscillometric finger-pressing method in smartphone encasings, which are commonly used to protect the phone against damage due to drops and otherwise or within the phones themselves. For example, a thin filmed force sensor could be placed on top of an existing PPG sensor on the back of the phone.

Other cuff-less BP measurement modalities are being widely pursued at present. Pulse transit time (PTT) is the most popular method (Mukkamala et al., 2015). PTT often varies inversely with BP in a person and can be measured simply as the relative timing between proximal and distal waveforms indicative of the arterial pulse. Hence, PTT could potentially permit convenient BP monitoring. However, PTT in units of milliseconds must be calibrated to BP in units of millimeters of mercury, and PTT, as a single value, cannot independently track systolic and diastolic BP. As a result, accuracy is the concern for the PTT-based approach. Ultrasound may allow for other methods. The most popular ultrasound method measures the arterial diameter waveform along

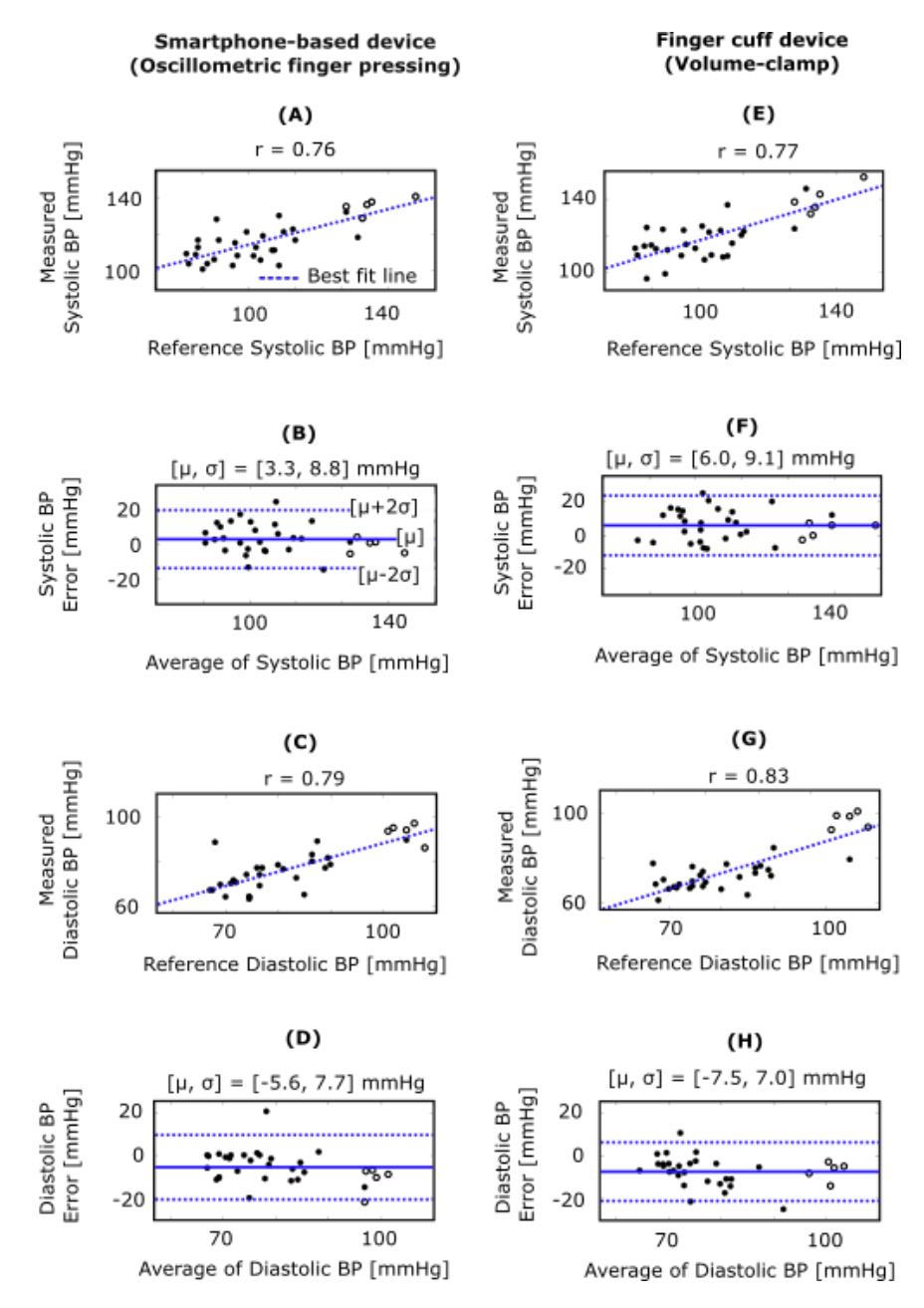


Figure 2.4: **Device accuracy results (n = 32 users).** Correlation and Bland-Altman plots comparing the brachial BP measurements from the smartphone-based device [oscillometric finger-pressing method (A to D)] and the brachial BP measurements from a finger cuff device [volume-clamp method (E to H)], with each relative to a standard arm cuff device. The filled circles are data points from new users holding both finger devices at the same height as the heart, whereas the unfilled circles are data points from experienced users holding both finger devices below the heart to raise the BP. r, correlation coefficient; μ , bias error (mean of the errors); σ , precision error (SD of the errors); solid line in Bland-Altman plots, bias error; dashed lines in Bland-Altman plots, limits of agreement.

with the local PTT (in the form of pulse wave velocity) and then applies the Bramwell-Hill equation to compute the absolute pulse pressure (systolic BP - diastolic BP) (Seo et al., 2015)(Beulen et al., 2011)(Vappou et al., 2011). Diastolic BP may also be measured via calibration of the PTT measurement. However, convenience is generally the concern for ultrasound systems. Arterial tonometry is a longstanding method (Pressman & Newgard, 1963) also worth mentioning. In theory, this method can measure a BP waveform without using a cuff by pressing a force sensor on an artery. The sensor must flatten or applanate the artery so that its wall tension is perpendicular to the probe. However, manual applanation and automatic applanation have proven to be difficult, so the measured waveform is routinely calibrated with cuff BP values in practice (Hansen & Staber, 2006).

The oscillometric finger-pressing method may overcome the shortcomings of other cuff-less BP measurement modalities. First, it can independently measure systolic and diastolic BP without any calibration and may therefore be sufficiently accurate. Second, it offers a convenience advantage over automatic cuff devices: People in low-resource settings may not have any access to cuff devices; others must go to pharmacies or other specified locations to use these devices; and people who own a device are unlikely to carry it with them wherever they go. By contrast, smartphones are readily available to many. About 3 billion people around the world are predicted to have smartphones by 2020 (Statista, 2019). It is also anticipated that smartphones will become widely used in low-income nations in the near future due to reduced costs resulting from more competition in the marketplace (Bastawrous & Armstrong, 2013). Furthermore, smartphones are constantly in use. For example, adults in the U.S. use these devices almost 3 hours a day on average (Curtin, 2018). An oscillometric method for cuff-less BP monitoring was previously proposed and was demonstrated in a pilot subject (Shaltis et al., 2008). In that study, a person raised her/his hand to lower the transmural pressure of the hand arteries via the hydrostatic effect while wearing a ring embedded with PPG and force sensors on a finger to measure the resulting variable amplitude blood volume oscillations and the pressure applied by the ring on the finger. The main concern with this interesting method is that the extent of the pressure reduction is limited by the arm length.

Hence, for most people, the ring must be applied on the finger at a pressure that does not deviate considerably from the mean BP of the person so that the oscillogram may be interrogated over the crucial zero–transmural pressure regime. Furthermore, extra sensors for measuring the height of the hand relative to the heart are required, or assumptions about the relative height must be made; motion artifact may be problematic when the hand raising is performed relatively quickly, or smooth muscle contraction may be a factor when the hand raising is performed very slowly (Pressman & Newgard, 1963); and hand-raising may be awkward for users in public settings. The proposed oscillometric finger pressing method overcomes these limitations, although it is vulnerable to BP measurement error when the device is not held at the same height as the heart.

We developed a smartphone-based device to implement the oscillometric finger-pressing method in real time. The prototype device includes a PPG and a force sensor unit to acquire the requisite measurements from the finger, a visual display on a smartphone application to guide the finger actuation, and an empirical algorithm to compute systolic and diastolic BP at the brachial artery from the finger measurements. It is BP at the brachial artery rather than the finger that is the proven cardiovascular risk factor (Lewington et al., 2002). The device outputs a try again message if the actuation is unsuccessful or the oscillogram quality is deemed inadequate. We tested the usability of the device and its accuracy against a standard automatic arm cuff device in 35 human subjects while likewise assessing a finger cuff device often used in research that has achieved approval from the U.S. Food and Drug Administration for measuring brachial BP (FMS, 2012). This finger cuff device applied the volume clamp method as follows. First, the finger cuff device slowly increases the cuff pressure while also measuring the blood volume via a PPG sensor within the cuff to compute mean BP according to the oscillometric principle. Then, the device continually varies the cuff pressure to maintain the "unloaded" blood volume (the blood volume at which the cuff pressure equals the mean BP) throughout the cardiac cycle via a fast servo-control system. The cuff pressure may therefore yield the finger BP waveform. This BP waveform is then converted to a brachial BP waveform via an empirical algorithm (Gizdulich et al., 1997).

We found that all new users could execute the finger actuation required by the smartphone-based

device and that most of these users could do so after one or two practice trials. We suspect that the finger actuation becomes second nature with increasing device usage. After the new users learned the finger actuation, the device yielded BP measurements much more often than not. When the device produced the try again messages, the cause was usually due to computation and measurement failures rather than actuation failure. Computation failures may be easily corrected in the future as more data are collected and with software updates. It may also be possible to reduce the frequency of try again errors due to measurement failure without compromising accuracy by lowering the standard for measurement quality. Although the device did not yield BP measurements in two users, the reason was computation failure for one of the users (and measurement failure for the other user).

The smartphone-based device could measure systolic and diastolic BP with promising accuracy. The device yielded bias and precision errors relative to the automatic arm cuff device that were close to the AAMI (Association for the Advancement of Medical Instrumentation) limits of 5 and 8 mmHg, but an AAMI data collection protocol was not used. Furthermore, the device measured BP as accurately as the finger cuff device. Here, all of the subjects used the device correctly. In practice, users may not always be so compliant. However, a key advantage of a smartphone-based BP monitoring device is that many measurements can be made over time with the ubiquitous system (Mukkamala & Hahn, 2018). These measurements could be averaged to eliminate error caused by random variations in finger placement on the sensor and in the height at which the device is held, as well as to mitigate error caused by imperfect BP computation. Averaging many measurements also abolishes the substantial BP variations that occur within a person due to stress, physical activity, recent ingestion of a meal, and other factors (Rosner & Polk, 1983). In this way, the device may be able to indicate a sufficiently reliable BP measurement for hypertension detection despite large errors in any single measurement. Screening for hypertension may be the main clinical application of the device, especially in the 20- to 50-year-old segment of the population who are often technology savvy and health conscious but may be at risk for early development of hypertension (Yano et al., 2015)(Weber, 2015). Our study has limitations, and future efforts

are needed to bring the oscillometric finger-pressing method to practice. One limitation is that the oscillometric finger-pressing method can neither make nighttime BP measurements, which are clinically important (Thijs et al., 2007), nor be performed by all people, such as those lacking fine motor control. However, even cuff-based methods may not be suitable for everyone (for example, morbidly obese people). Another limitation is that the smartphone based device was not tested according to an AAMI data collection protocol, which involves a subject population that covers a prescribed range of BP values (ISO, 2013). However, by also studying experienced users during a hydrostatic challenge, we were able to extend the tested range of each BP measurement to 40 to 50 mmHg. The device may be improved by leveraging additional sensing to confirm correct device usage, by mitigating the adverse effect of finger vascular tone changes via inclusion of a temperature sensor to assess cold-induced finger vasoconstriction, or by applying a physics-based algorithm to compute both BP and the arterial compliance curve (rather than an empirical algorithm, which may implicitly assume invariant arterial compliance curves despite finger vascular tone changes) (Li et al., 2017). The smartphone could also warn users of high BP, securely transmit the measured BP to caregivers, and send text reminders to patients with uncontrolled BP to take their medications.

2.4 Materials and Methods

2.4.1 Study design

We investigated the oscillometric finger-pressing method for cuff-less BP monitoring using a smart-phone. We performed informal and formal human studies under protocols approved by the Michigan State University Institutional Review Board and with written, informed consent from each subject. The informal study facilitated the development of a single prototype device, whereas the formal study allowed for objective testing of this device. The formal study followed a prospective design, in which the real-time output of the device was assessed (as opposed to a retrospective design in which an offline output, as determined by first recording the finger blood volume oscillation and pressure measurements of the device and then analyzing the measurements, is assessed). The study was therefore necessarily blinded to all cuff BP measurements. This study included the following

predefined components: number of subjects (n = 35) that is about half of the AAMI study population (28) and comparable to similar studies in the field for demonstrating proof of concept (Mukkamala et al., 2015); number of measurements per subject; and subject and data inclusion/exclusion criteria. No outliers were excluded.

2.4.2 Device development

2.4.2.1 Informal human study

To develop the hardware component of the device and a basic visual display for finger actuation guidance, we qualitatively explored various options in about 10 human subjects. We then collected a training data set to define the software component of this device, including finger measurements, via the device held at the same height as the heart and reference BP measurements via a standard automatic arm cuff (BP7650N, Omron) from 31 human subjects (age, 31 ± 7 years; height, 170 ± 8 cm; weight, 68 ± 10 kg; 39% females). Reference systolic and diastolic BP in this data set ranged from 90 to 124 mmHg and 60 to 89 mmHg, respectively. We computed reference mean BP, which was not outputted by the automatic arm cuff device, from systolic and diastolic BP according to the 0.4/0.6 rule (Bos et al., 2007).

2.4.2.2 Prototype Hardware

We built a physical device consisting of a 3D-printed case attached to a smartphone. The case (Vero White material; 112 mm × 68 mm × 11.6 mm dimensions; printed by Objet350 Connex, Stratasys) was attached using screws to the back of a standard smartphone encasing (SAMS6HPCTUFF2DIM1, MyBat), which housed the smartphone (Galaxy S6, Samsung). The components within the case include a sensor unit, data acquisition and transmission circuitry, and a power supply, as shown in Fig. 2.5. The sensor unit consists of PPG and force transducers. The PPG sensor was custom-built, comprising a light-emitting diode and photodetector pair op-

erating in reflectance-mode and at an infrared wavelength (940 nm) to penetrate beneath the skin (Mukkamala et al., 2015) and to provide superior signal quality in lower–skin perfusion conditions (dark skin pigmentations and cold temperatures) (Lemay et al., 2014). The sensor surface, which constitutes the finger pressing area, is a 10-mm-diameter circle. The force sensor (CS15-4.5N, SingleTact) is a thin-filmed, capacitive transducer that measures normal direction force, with specifications congruent with BP measurement (0.9 mmHg resolution and 430 mmHg range). The force-sensitive area is a 15 mm diameter circle. The PPG sensor is positioned on top of the force sensor with a rigid-structure-rubber sheet (TangoBlack material; 15 mm diameter) between the two, which allows the force applied on the PPG sensor, but not elsewhere on the case surface, to reach the force-sensitive area and be uniformly distributed on it. A one-time calibration of the force sensor was performed while residing in the completed case via placement of high-density weights (WHST13, United Scientific Supplies) on the PPG sensor. The relationship from the voltage (V) measured by the force sensor to the known pressure (P, the force exerted by each weight divided by the area of a 10 mm diameter circle) was represented with a piece-wise linear function (P = 560.1V - 281.9ifV < 0.74 or P = 225.2V - 32.1 otherwise). The blood volume waveform outputted by the PPG sensor is amplified and filtered via a band-pass filter with cutoff frequencies of 1.8 and 4.3 Hz (analog signal conditioning) to differentiate the blood volume waveform with respect to time while also attenuating high-frequency noise. The applied pressure outputted by the force sensor is conditioned using circuitry provided with the sensor. The two measurements are then passed through an analog-to-digital converter (ADS1115, Adafruit) with 16-bit resolution and at a 40 Hz sampling rate. The digital signals are finally transmitted to the smartphone via a development board with a processor (ATSAMD21G18, Arm) interfaced to a Bluetooth low energy module (nRF51822, Nordic Semiconductor). All components are powered with a rechargeable lithium-ion polymer battery (3.7 V, 150 mA·hour), and switches are included to shut down the battery and sensors.

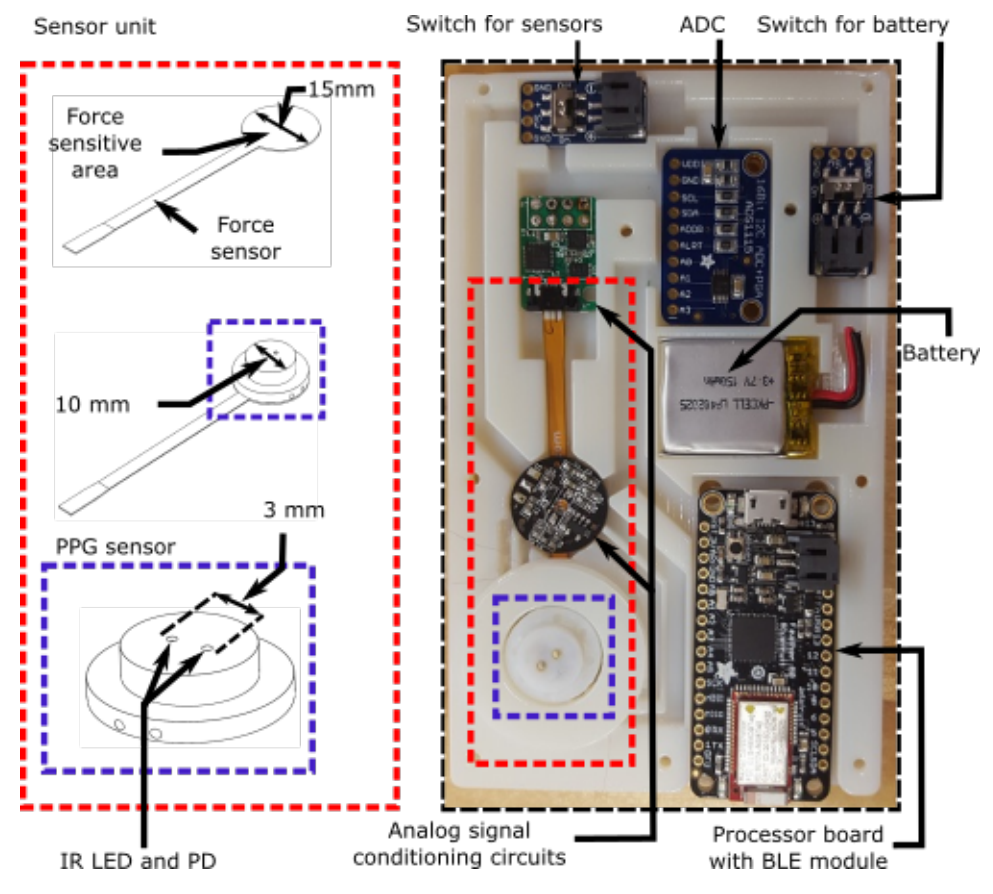


Figure 2.5: **Smartphone-based device hardware.** Schematic diagram of the PPG and force sensor unit and photograph of this unit, data acquisition and transmission circuitry, and power supply housed within the 3D-printed case affixed to the back of the phone. IR, infrared; LED, light-emitting diode; PD, photodetector; ADC, analog-to-digital converter; BLE, Bluetooth low energy.

2.4.2.3 *Software*

We created an Android application to run on the smartphone. Fig. 2.6 shows a flow chart of the application along with the important equations for computing BP. The application includes a visual display to guide the finger actuation and an algorithm to compute and output BP or ask the user to try again. The application uses various thresholds and BP computation formulas that were defined on the basis of the training data set. Formulas that optimized the agreement between the smartphone-derived BP measurements and the reference arm cuff device measurements were selected. Thresholds were selected qualitatively by choosing what we considered to be reasonable values and then by confirming that these values allowed for what we considered to be a good

balance between BP measurement accuracy and percentage of try again messages. The visual display depicts separate graphs of the blood volume waveform and applied pressure both plotted against time. Each sample of these measurements is displayed on its respective plot as it is being acquired. The applied pressure displayed specifically represents a 1-s moving average. The applied pressure versus time plot also includes a pair of blue lines, indicating a target rate range of 4.7 to 6.0 mmHg/s for the pressure increase. The magnitude of the blood volume oscillations is monitored in real time via a 1.33 s moving average of the SD of the blood volume waveform. If this SD falls below 20% of its maximum attained value, then the measurement automatically terminates because enough data have been obtained. Moreover, if three successive samples of the applied pressure fall outside of the two target blue lines, then the application will ask the user to try again. The algorithm first constructs the oscillogram from the zero-mean blood volume waveform and the applied pressure obtained during a successful finger actuation. The measurements are analyzed over the time interval for which the applied pressure ranges from 40 mmHg to the termination pressure (TP). The average heart rate is determined from the blood volume waveform based on its spectral peaks within the frequency range of 0.5 to 3 Hz. The peaks of each beat of the blood volume waveform are then detected by leveraging the average heart rate and the local maxima of the waveform. Because the PPG sensor measures a differentiated blood volume waveform, the waveform peaks are reflective of the peak-to-peak amplitudes of the blood volume oscillations. If the average of the reciprocal of the peak-to-peak intervals is not within 10% of the average heart rate determined via spectral analysis (in hertz), then the application will ask the user to try again because the blood volume waveform may be contaminated by artifact or the waveform beats may not have been well detected. The applied pressure measurement is thereafter smoothed via a third-order polynomial fit. A discrete oscillogram is then formed by plotting the blood volume peaks versus the corresponding pressure and smoothing the plot via a three point moving average. A final, continuous oscillogram is constructed by fitting the parametric function in Eq. 1 in Fig. 2.6 to the discrete oscillogram. In this equation, x and y are the abscissa and ordinate, respectively, of the oscillogram, and A_i and B_i are the parameters that define the oscillogram. This equation

models the oscillogram as an asymmetric function, as justified elsewhere (Liu et al., 2017), via two half Gaussian functions. As illustrated to the right of Eq. 1 in Fig. 2.6, the parameter A_2 represents the starting value of the oscillogram; A_1 and B_1 represent the maximal amplitude of the oscillogram and the applied pressure at which it is maximal, respectively; and \emph{B}_2 and \emph{B}_3 represent the width of the oscillogram over the pressure range to the left and right of its maximum, respectively. Note that the parameter A_2 is needed, because the device asks the user to maintain a relatively constant pressure before beginning the actuation such that the oscillogram is often flat initially. These five parameters are estimated via nonlinear least-squares fitting. The algorithm then computes BP from the final oscillogram or asks the user to try again. Empirical methods are used, similar to cuff-based devices that use fixed-ratio or similar methods to compute brachial BP from an arm oscillogram (Alpert et al., 2014) (Van Montfrans, 2001). In the fixed-ratio method, mean BP is first obtained as the cuff pressure at which the oscillogram is maximal, and systolic and diastolic BP are then determined as the cuff pressure at which the oscillogram is some fixed ratio of its maximal value. Similarly, finger cuff devices based on the volume-clamp method convert the measured finger BP to brachial BP via a population average transfer function and a regression equation (Gizdulich et al., 1997). The brachial BP values are specifically computed from the finger oscillogram model parameters via the empirical linear regression formulas in Eqs. 2 to 4 in Fig. 2.6. We arrived at these formulas using stepwise regression, which determined both the model parameters that are statistically significant regressors (P < 0.05) of the reference cuff BP values and the associated coefficients in the regression model for computing BP. The diastolic BP formula is conceptually similar to the fixed-ratio method, and the constant term therein also accounts for brachial diastolic BP being systematically higher than finger diastolic BP (Gizdulich et al., 1997)(Wesseling et al., 1985). The mean BP formula includes both B_1 and A_2/A_1B_2 (which is a measure of oscillogram width) and is therefore similar to an existing method designed to handle relatively flat or wide oscillograms, in which the mean BP is determined as the lowest external pressure at which the oscillogram is still close to maximal (Ursino & Cristalli, 1996). The constant term in the formula likewise accounts for brachial mean BP being systematically higher than finger

mean BP (Gizdulich et al., 1997)(Wesseling et al., 1985). The systolic BP formula is based on the 0.4/0.6 rule for computing brachial mean BP from brachial systolic and diastolic BP (Bos et al., 2007). Although stepwise regression yielded a different formula for systolic BP, the degree of significance of the regressors was borderline ($P \cong 0.05$). Furthermore, the difference between brachial systolic BP and finger systolic BP is not only due to the resistive pressure drop but also due to arterial wave reflection and is therefore more complicated. Hence, the simple formula here may generalize better. Finally, as shown to the left of Eqs. 2 to 4 in Fig. 2.6, if B_2 or B_3 is greater than 100 mmHg (the oscillogram is excessively wide), A_2 is less than 0 or greater than A_1 (the oscillogram is negative or monotonically decreasing), the oscillogram amplitude at an applied pressure of 40 mmHg (y_{40}) is greater than $0.8 * A_1$, or the oscillation amplitude at the TP (y_{TP}) is greater than $0.5 * A_1$ (the oscillogram has not been interrogated over a sufficiently wide pressure range), then the application will not output BP and instead will ask the user to try again. Note that these empirical thresholds and formulas are expected to change because more data are added to the training data set.

2.4.3 Device testing

2.4.3.1 Formal Human Study

We prospectively tested the smartphone-based device for usability and accuracy against a standard automatic arm cuff device. We recruited 30 users who had not used the device before and 5 experienced users. These five users were part of the training data set subject cohort but performed an intervention to change their BP. The inclusion criteria were: (i) from ages 21 to 60 years; (ii) right-handed (because the device was designed for such users but could be easily extended for both right- and left-handed users); (iii) no cardiovascular disorders other than hypertension; and (iv) no problems with fine motor control. The exclusion criterion for the accuracy testing was invalid automatic cuff BP measurements defined as: (i) a poorly fit cuff on the user's arm or (ii) cuff BP measurements (mean via 0.4/0.6 rule) deviating by > 10 mmHg (because BP was assumed to be stable throughout the protocol). Only one user was excluded because of invalid cuff BP

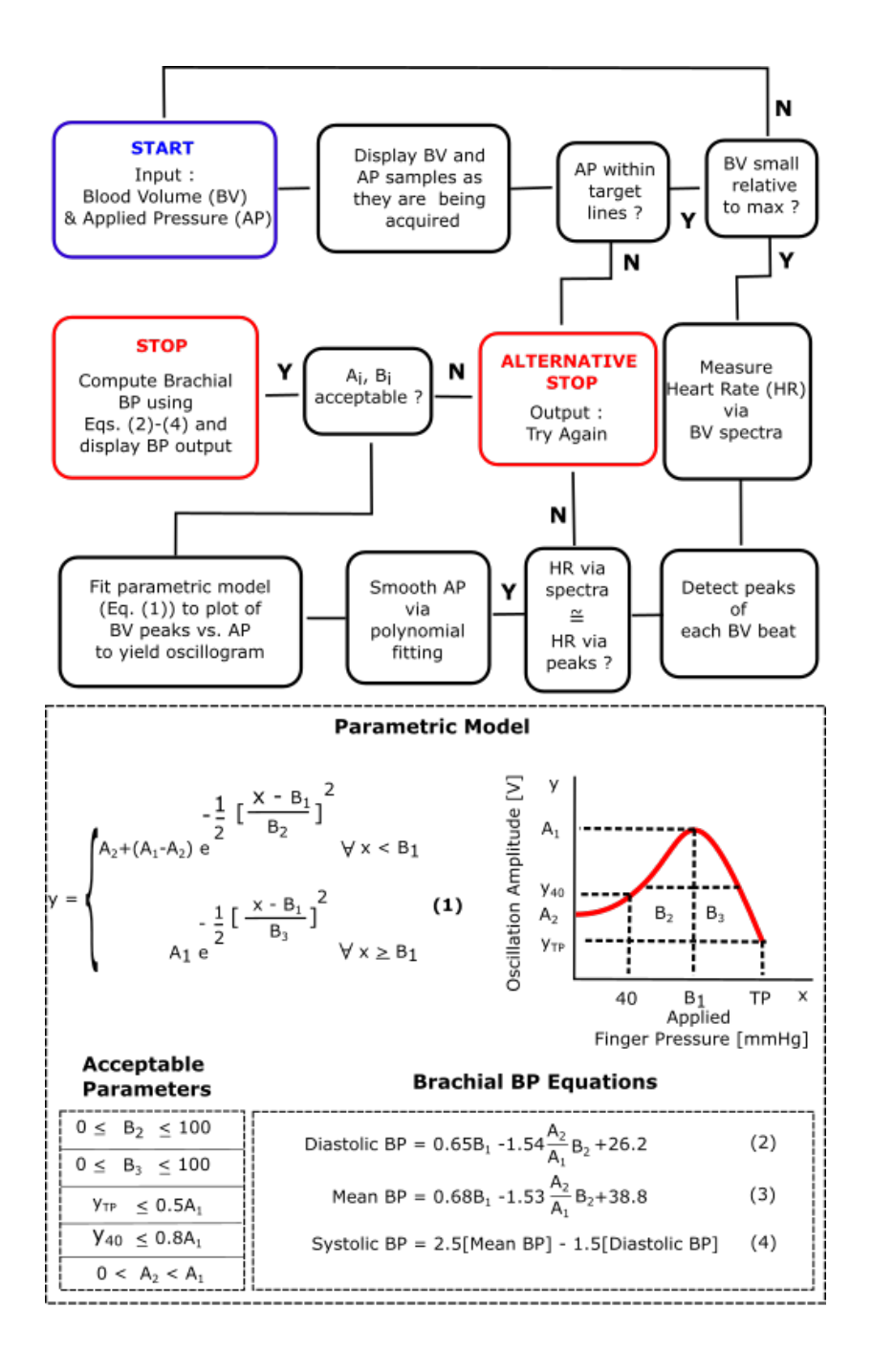


Figure 2.6: **Smartphone-based device software.** Flowchart of the smartphone application and important equations for computing BP running on the phone wherein the input is the measured blood volume waveform and applied pressure and the output is brachial BP values or a try again message. The blue box indicates the beginning of the flowchart, whereas the red boxes indicate the two possible ends of the flowchart. The plot illustrates a parametric model of the oscillogram [blood volume oscillation amplitude (y) as a function of the applied finger pressure (x)] from which BP is computed. BP computation details are provided in the "Software" subsection of Materials and Methods.

measurements.

2.4.3.2 Experimental Measurements and Protocol

Figure 2.7 shows the BP measurement devices and protocol. The BP measurement instruments were the smartphone-based device (Fig. 2.7(A)), a standard oscillometric arm cuff device (BP7650N, Omron; Fig. 2.7(B)), and a finger cuff device based on the volume-clamp method that transforms a measured finger BP waveform into a brachial BP waveform (Finometer Model 2, Finapres Medical Systems; Fig. 2.7(C)). The protocol included an initial learning phase (for new users only) and a data collection phase (for all users; Fig. 2.6(D)). During the learning phase, use of the smartphonebased device was demonstrated, and users were allowed to practice with the device until they were able to perform the index finger actuation correctly in terms of keeping the applied finger pressure between the target blue lines. During the data collection phase, a series of BP measurements were made as follows: BP with the standard cuff device placed properly on the right arm; multiple cuff-less BP measurements using the smartphone-based device with at least 1 min between each measurement; brachial BP waveform with the finger cuff device for 1 min, with the cuff positioned on the index finger of the right hand; and BP with the standard arm cuff device. Smartphone data collection was terminated once (i) two measurements yielded mean BP values within 10 mmHg; (ii) three measurements produced BP values; or (iii) four measurements were made. New users held the smartphone based device and finger cuff device at the same height as the heart, whereas the experienced users (n = 5) held both devices at the same height but well below the heart to raise their BP via the hydrostatic effect. The finger cuff device also included a sensor to measure the BP offset caused by the hydrostatic effect ($\rho g h$, where ρ is blood density, g is gravity, and h is the height between the heart and finger).

2.4.3.3 Data Analaysis

To test usability, we recorded the number of practice trials required for each new user to successfully execute the finger actuation, documented the number of BP values obtained and try again messages

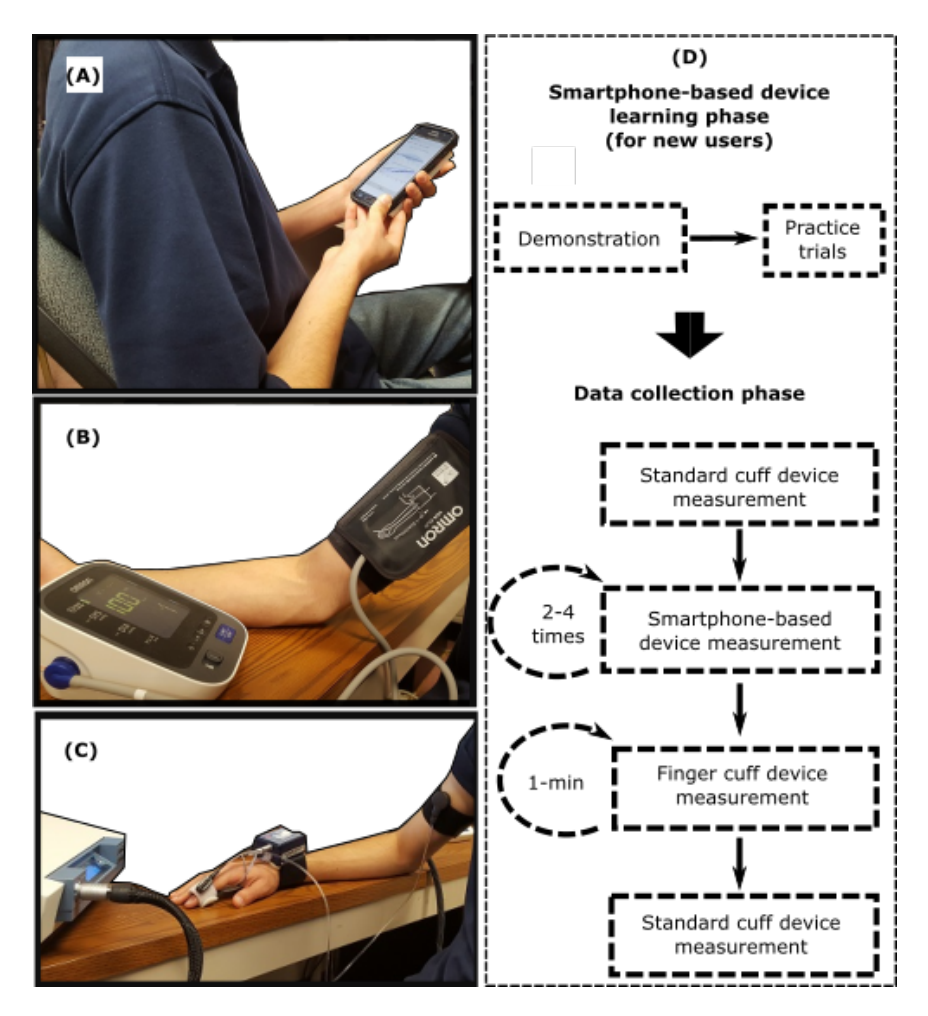


Figure 2.7: **Human study design for device testing.** Photographs of the three BP measurement devices for study: (A) the smartphone-based device, (B) a standard automatic arm cuff device (the reference device), and (C) a finger cuff device (a competing device). (D) Diagram of the experimental protocol for BP measurement using the devices shown in (A) to (C). The protocol included a learning phase for new users to become familiar with the smartphone-based device and a data collection phase involving a measurement with the reference device, two to four measurements with the smartphone-based device, 1 min of measurement with the finger cuff device, and a final measurement with the reference device. Study details are provided in the "Device testing: Formal human study" subsection of Materials and Methods.

outputted by the device for each of the users, and determined the reason for each of the try agains via post hoc visual inspection of the data. To test accuracy, we averaged the cuff-less BP measurements of the smartphone-based device when multiple measurements were available for the user and averaged the pair of measurements from the arm cuff device. For the experienced users, we then added the ρgh measurement to the systolic and diastolic BP measurements from the arm cuff device. We did not assess the mean BP measurements from the smartphone-based device because the reference device did not output this BP value, and use of the 0.4/0.6 rule for computing reference mean BP may bias the results.

2.4.3.4 Statistical analysis

We used standard analyses to assess the systolic and diastolic BP measurements of the smartphone-based device against the reference BP measurements from the arm cuff device. In particular, we assessed the accuracy visually using correlation and Bland-Altman plots and quantitatively using the correlation coefficient (r), bias error (μ , mean of the errors), and precision error (σ , SD of the errors). For comparison, we assessed the average brachial BP values obtained using the finger cuff device against the reference BP measurements from the standard cuff device. The results of the devices were similar enough that statistical comparisons were not necessary (Fig. 2.4).

2.5 Conclusion

In summary, we studied the oscillometric finger-pressing method for cuff-less BP monitoring using a smartphone. Although various form factors for implementing this method may be envisaged, the smartphone form may allow the method to reach the most people while being conveniently housed within a single, portable device. In this way, a complete hypertension management system would be available in the pockets of many.

CHAPTER 3

AN IPHONE APPLICATION FOR BLOOD PRESSURE MONITORING VIA THE OSCILLOMETRIC FINGER PRESSING METHOD

3.1 Introduction

High blood pressure (BP) is a major, modifiable cardiovascular risk factor (Lewington et al., 2002)(Psaty et al., 1998), yet hypertension awareness and control rates are low (Ibrahim & Damasceno, 2012). Ubiquitous BP monitoring could improve these rates, but existing devices require inflatable cuffs and thus do not afford such monitoring. While cuff-less BP measurement methods are being widely pursued, many of the methods require calibrations with cuff BP measurements(Mukkamala et al., 2015)(Mukkamala & Hahn, 2018).

Recently, we proposed a method for cuff-less and calibration-free BP monitoring via a smart-phone(Chandrasekhar et al., 2018a). The method represents an extension of the time-honored oscillometric cuff BP measurement principle. The idea is for the user to serve as the actuator (instead of the cuff) by pressing her fingertip against the phone to steadily increase the external pressure of the underlying artery, while the phone, embedded with photoplethysmography (PPG) and force transducers, serves as the sensor (rather than the cuff) to measure the resulting variable-amplitude blood volume oscillations and applied pressure. The phone also visually guides the finger actuation and then computes BP from the measurements just like a cuff device. We developed a device in the form of a custom PPG-force sensor unit affixed to the back of a smartphone to implement the "oscillometric finger pressing method" and showed that the device can be usable and accurate compared to cuff devices. However, the need for special sensors above and beyond the smartphone limits the accessibility of the method.

Here, we developed a smartphone application that leverages PPG and force sensors already in the phone to implement the oscillometric finger pressing method. We then tested the application against cuff BP measurements for a proof-of-concept demonstration.

3.2 Results

3.2.1 iPhone Application

Fig. 3.1(a) illustrates the oscillometric cuff BP measurement principle, and Fig. 3.1(b) shows the application developed to extend the principle to measure BP with the latest iPhone (X model). The front of this phone is all screen, except for a small notch that includes the camera for taking "selfies". The application employs this front camera as the PPG sensor where the light source is ambient light and/or screen light (bright setting, which we anecdotally found to suffice in the dark). Spatial averaging followed by band-pass (1.8–4.3 Hz) filtering of the red video channel is applied to extract the blood volume oscillations. The application employs the strain gauge array under the phone screen (but not the notch) for employing "peek and pop" via "3D Touch" (Chamary, 2017) as the force sensor. Apple's UIKit is used to extract the strain gauge output(Apple, 2018). Through placement of high density weights on the screen adjacent to the camera, the application derives force (F, grams) from the strain gauge out- put (V) as F = 443.75V, where V takes on 400 levels from 0 to 0.83 (firm setting). Like our previous device(Chandrasekhar et al., 2018a), the application plots the data as they are recorded to visually guide the finger actuation. Fig. 1c shows that the application also includes measurement of the user fingertip dimensions. One purpose of this measurement is to guide fingertip placement on the screen when measuring BP such that the underlying transverse palmar arch artery (at about the middle of the fingertip) is above the camera. Another purpose is to estimate the finger pressing contact area on the screen, which is needed to compute finger pressure as force divided by area. This measurement need only be made once per user, as finger dimensions and pressing contact area hardly change throughout adulthood(Wu, 2008). Based on a training dataset comprising index fingertip width and height measurements via the application and reference finger pressing contact area measurements via fingerprinting from 20 subjects, the screen finger pressing contact area (A, mm²) is calculated as A = 0.56wh - 5.67, where w and h are specifically the fingertip width at the base of the nail and half the height of the fingertip starting from the crease at the top knuckle minus 2.7 mm (distance from the camera center

to the screen edge). Note that the finger- prints were obtained during firm pressing and may thus be valid around the maximum blood volume oscillation regime, which includes mean BP and is mainly used for BP computation(Liu et al., 2016). Based on fingerprint dimensions from thousands of subjects(Wu, 2008) and the force measurement specifications above, we estimate that 95% of people could achieve finger pressure at maximum of >178 mmHg and resolution of <2 mmHg with the application. These specifications are largely congruent with BP measurement.

3.2.2 Usage

The user initializes the application by placing her index fingertip so that the crease at the top knuckle is aligned with the black horizontal line (Fig. 3.1(c)). The user or another person then moves the red vertical and horizontal lines to measure the fingertip width and height (Fig. 3.1(c)). The user may then measure BP, as shown in Fig. 3.1(d). The user places her fingertip so that it is tightly encompassed by the rectangular box of width w and height h near the camera when viewing from directly above; holds the phone horizontally at heart level while resting her fingertip flat on the phone for uniform, normal direction force application; and presses to keep the finger pressure within the target blue lines until enough data have been obtained. Using the algorithm employed by our previous device(Chandrasekhar et al., 2018a), brachial BP is then computed from the finger measurements or a try-again message is outputted.

3.2.3 Accuracy

We tested the iPhone application in 20 different subjects. These users were mainly from the cohort employed for testing our previous device (to facilitate comparisons) and included four experienced users of the application. Each new user performed three to six practice trials followed by four measurements. Each experienced user performed two measurements holding the phone well below heart level to raise BP and two normal measurements. The application yielded BP in about half the measurements for the new users and outputted BP in 18 of the users. However, the application did not yield BP in the other two users due to poorly estimated finger pressing contact area (29–43%

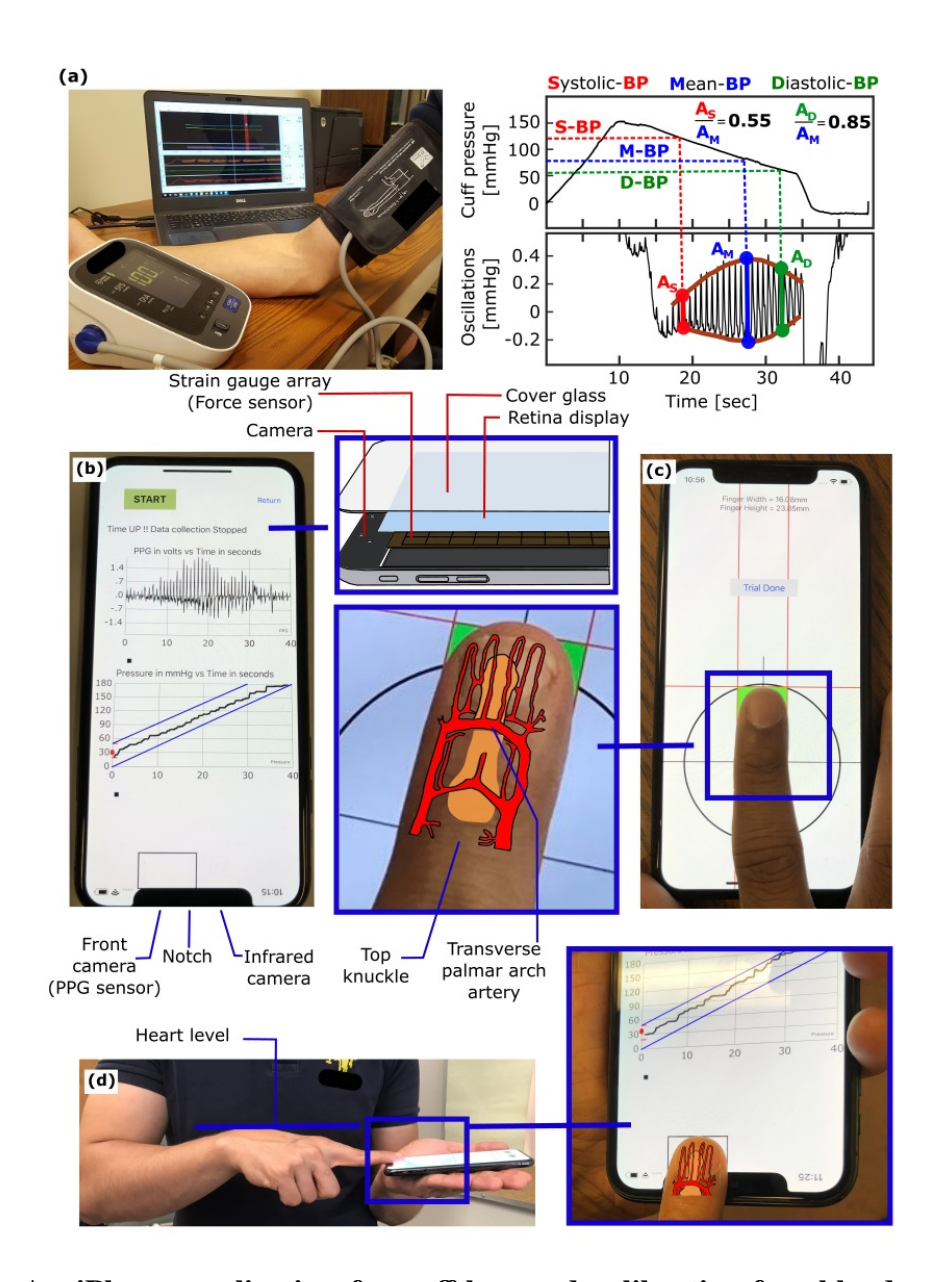


Figure 3.1: An iPhone application for cuff-less and calibration-free blood pressure (BP) monitoring via extension of the oscillometric cuff measurement principle. (a) Photograph of an oscillometric cuff device and diagram of BP computation from the measured cuff pressure and blood volume oscillations. Reproduced from ref.6. (b) Photograph of an iPhone X application to implement the "oscillometric finger pressing method" by measuring finger pressure via the strain gauge array under the screen and finger blood volume oscillations via the front camera. Insert redrawn from (Chamary, 2017) (c) Photograph of a user initializing the application by measuring fingertip width and height from the top of the fingertip to the artery near the middle of the fingertip. (d) Photograph of the user making a measurement by placing the fingertip within a rectangular box of the measured width and height; holding the phone horizontally at heart level while resting the fingertip flat on the phone; and pressing to increase the pressure within the two target blue lines.

error relative to fingerprinting compared to <7% mean absolute error in the 18 subjects). The BP measurements from each new user and experienced user holding the device below the heart were averaged and assessed against BP measurements from a standard arm cuff device. Fig. 3.2(a–d) shows correlation and Bland-Altman plots for the systolic and diastolic BP measurements from the 18 users. The bias errors (μ) and precision errors (σ) of the application were -4.0 and 11.4 mmHg for systolic BP and -9.4 and 9.7 mmHg for diastolic BP over about a 50 mmHg range of BP. Fig. 3.2(e–h) shows corresponding plots for a finger cuff device, which is FDA-cleared for measuring brachial BP11. The application showed errors that were only about 2 mmHg higher on average than the finger cuff device.

3.3 Discussion

The iPhone application errors are close to our previous deviceChandrasekhar et al. (2018a). However, the application did not yield BP in two users due to finger pressing contact area misestimation, which is not a factor for the device. The application also yielded more try-again messages (about 50 versus 40%) and less repeatable BP measurements (e.g., mean absolute difference between successive measurements at heart level of about 7 versus 5 mmHg) likely due to variability in fingertip positioning despite the rectangular box guide. Hence, not surprisingly, the application may be less effective than our device, which employs application-specific sensors. However, any reduction in effectiveness may be offset by the increased accessibility of a smartphone application. An estimated 50 million iPhone X models have already been sold(Reisinger, 2008). Moreover, other smartphones have 3D Touch capability including iPhone models 6S and higher7 and the Huawei Mate S model(Daniil, 2015). Hence, applications for these phones may likewise be developed (with appropriate modifications for differing arrangements of the camera/PPG sensor and screen). In 2017, 328 million iPhones with 3D Touch capability (excluding iPhone 8 and X) were being used(Statista, 2018). Hence, it is conceivable that the oscillometric finger pressing method could reach about 500 million smartphones already in use. Our iPhone application should be improved. Most importantly, the finger pressing contact area was mis-estimated in two subjects and variably

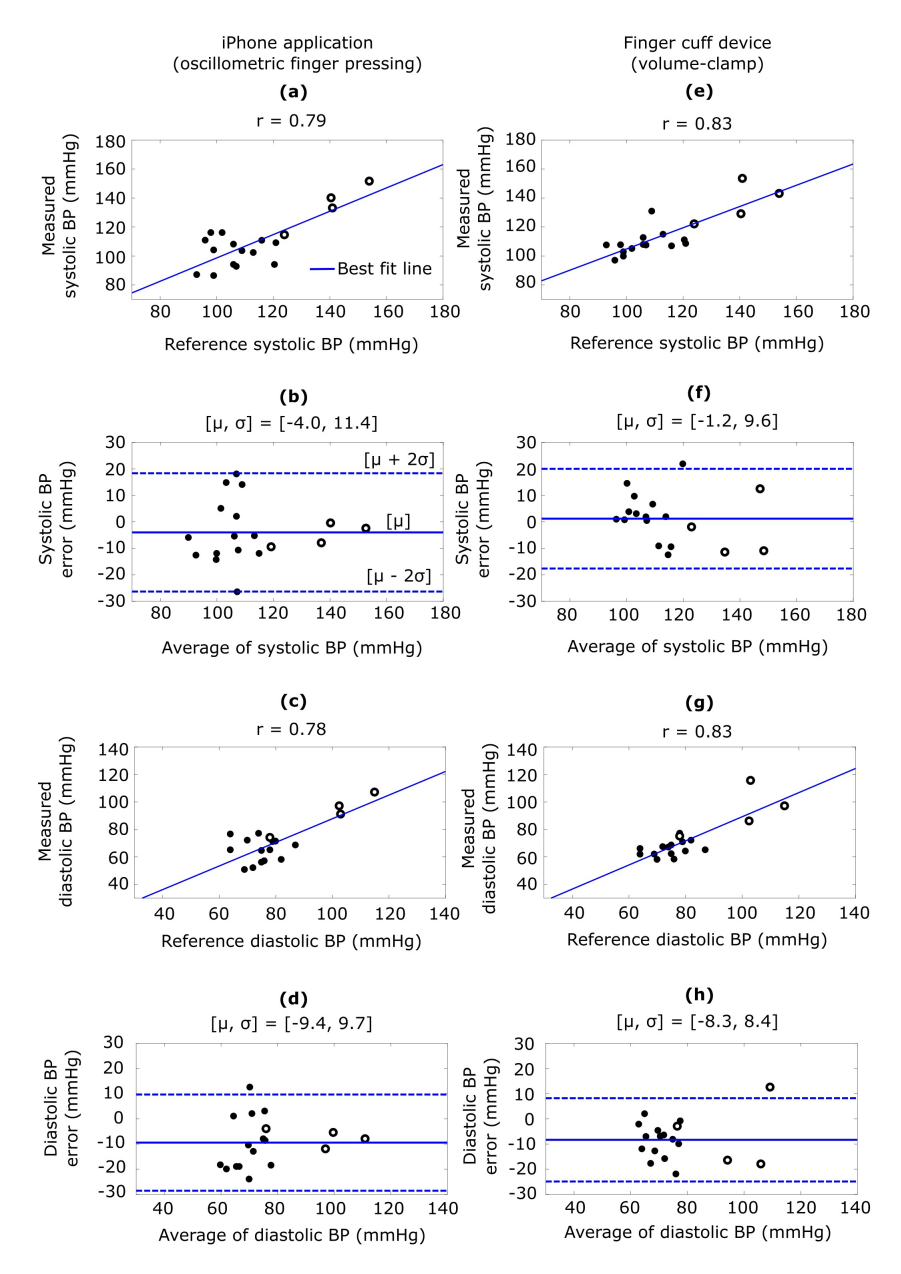


Figure 3.2: **Application accuracy results** ($\mathbf{n} = 18$ users). Correlation and Bland-Altman plots comparing the brachial BP measurements from the (a–d) iPhone application and (e–h) a finger cuff device to the brachial BP measurements from a standard arm cuff device. The closed circles are data from new users holding the finger devices at heart level, and the open circles are data from experienced users holding the finger devices below the heart to increase BP. r, correlation coefficient; μ , mean of errors (bias error); σ , standard deviation of errors (precision error).

estimated in some other subjects due to fingertip mis-positioning. In practice, when the application consistently outputs try-again messages or unusual BP measurements, the area could be determined with just one cuff BP measurement (as opposed to periodic cuff calibrations required by competing methods (Mukkamala et al., 2015)(Mukkamala & Hahn, 2018)). The application could also output a running average of the past several BP measurements (instead of individual BP measurements) to mitigate random variability resulting from fingertip mis-positioning and other factors(Mukkamala & Hahn, 2018). In this way, the application may be able to yield BP errors that are closer to the putative bias and precision error limits of 5 and 8 mmHg(ISO, 2013) than the results reported herein. However, there may be better solutions. One possibility is to measure the area (even at different finger pressures) via the fingerprint sensor under the screen for authentication in upcoming smartphones including the 2019 iPhone X16,17. The optimal solution is if Apple were to provide access to an accurate area measurement as the user performs the actuation via the capacitive sensor array also under the screen(Chamary, 2017). Such access may be possible, as superior area assessment may be obtained with Android devices. In addition, the infrared camera also on the notch of the iPhone X (Fig. 3.1b) for authentication may be used to provide higher-fidelity blood volume oscillations in cold and other low signal conditions (Lemay et al., 2014). Finally, the BP computation algorithm needs further development to satisfy the accuracy requirements of a regulatory test(ISO, 2013).

3.4 Materials and Methods

We performed two sets of human studies under protocols approved by the Michigan State University Institutional Review Board and in accordance with relevant guidelines and regulations. We obtained written, informed consent from each subject. The purpose of the first study was to develop the iPhone application and a method for estimating the finger pressing contact area in particular. The purpose of the second study was to conduct a proof-of-concept evaluation of the application against cuff devices. Note that the application did not output BP or a try-again message in real time for the sake of convenience (as the BP computation algorithm of our previous device was

implemented as an Android application(Chandrasekhar et al., 2018a) instead of an iOS application needed here). We thus applied the code for the BP computation algorithm of the previous device offline to the finger measurements from the application while blinded to the cuff BP measurements.

3.4.1 Application Development

We studied 22 healthy subjects (age, 27 ± 3 years; height, 169 ± 12 cm; weight, 73 ± 11 , kg; 45% females). For each subject, we took two or three measurements of the fingertip "rectangular box" width and height (w and h, as defined in the main text) via the application and three fingerprints via an inkpad and graph paper. For each fingerprint, the subject pressed firmly and uniformly in the normal direction. We averaged the w (mm) and h (mm) measurements and computed the reference finger pressing contact area (A, mm²) as the average of the number of squares of fingerprint ink on the graph paper that were 2.7 mm above the middle of the fingertip (see rationale in the main text). We plotted A versus each of w, h, and w·h. After excluding two outlier data points, each set of 20 data points appeared to be well fit by a line. We found that A was best predicted from w·h (see line formula presented in the main text).

3.4.2 Application Testing

3.4.2.1 Experimental Protocol

We studied 20 different subjects (age, 33 ± 10 (18–55) years; height, 169 ± 7 cm; weight, 66 ± 10 , kg; 45% females). This number of subjects is congruent with many other published studies on cuff-less BP measurement(Mukkamala & Hahn, 2018). We recruited most of these subjects from the cohort employed for testing our previous device(Chandrasekhar et al., 2018a). Sixteen of the subjects had never used the iPhone application, whereas the other four subjects were experienced users of the application. The inclusion criteria were: (i) ages 18 to 60 years and (ii) normotensive or hypertensive. The exclusion criteria were (i) cardiovascular disorders other than hypertension or (ii) problems with fine motor control. We commenced study of each subject by making the

same measurements as the first human study. However, in this evaluation study, the application estimated the finger pressing contact area by applying the average of the w and h measurements to the line formula. For the new users, we then gave demonstrations on how to use the application to make finger measurements. We allowed them to perform three to six practice trials. We concluded study of each subject with a series of measurements as follows. We obtained three reference BP measurements via a standard oscillometric arm cuff device (BP786, Omron, Japan). We then had the new users make four finger measurements with the iPhone application and the experienced users make two finger measurements while holding the phone well below heart level to raise BP. We next measured the brachial BP waveform with a finger cuff device based on the volume-clamp method (Finometer Model 2, Finapres Medical Systems, The Netherlands). We thereafter obtained two more reference BP measurements using the standard cuff device. We also had the experienced users make two more measurements while holding the phone at heart level at a later time.

3.4.2.2 Data Analysis

We applied the same code employed by our previous device(Chandrasekhar et al., 2018a) off-line to compute brachial BP from the entire finger blood volume oscillation and pressure recordings from the application or output a try-again message. We documented the number of BP measurements and try-again messages. We averaged all BP measurements from the iPhone application for each new user and each experienced user holding the device below the heart and averaged the last four BP measurements from the arm cuff device. For the experienced users, we added a ρ gh measurement provided by the finger cuff device (where ρ is the known blood density (near that of water), g is gravity, and h is the vertical distance between the heart and device) to the systolic and diastolic BP measurements of the reference arm cuff device. We also likewise measured the reference finger pressing contact area via the fingerprinting. As in our previous study(Chandrasekhar et al., 2018a), we used standard analyses to assess the systolic and diastolic BP measurements from the iPhone application as well as the finger cuff device, each against the reference BP measurements from the arm cuff device. We assessed accuracy qualitatively in terms of correlation and Bland-Altman

plots and quantitatively in terms of the correlation coefficient (r), bias error (μ , mean of the errors), and precision error (σ , standard deviation of the errors). We also assessed BP measurement repeatability via the mean absolute difference of successive measurements at heart level per subject in mmHg and evaluated the finger pressing contact area estimates via the mean absolute difference relative to the reference measurements in percent. Note that we only assessed the repeatability of BP measurements made with the iPhone at heart level, as it was not easy to perform BP measurements with the device well below the heart.

3.5 Conclusion

In summary, this proof-of-concept study surprisingly indicates that cuff-less and calibration-free BP monitoring may be feasible with many existing and forthcoming smartphones by leveraging sensors built-in for other purposes. Such ubiquitous BP monitoring may improve hypertension awareness and control rates and thereby help reduce the incidence of cardiovascular disease and mortality

CHAPTER 4

FORMULAS TO EXPLAIN POPULAR OSCILLOMETRIC BLOOD PRESSURE ESTIMATION ALGORITHMS

4.1 Introduction

Oscillometry is the blood pressure (BP) measurement methodology of most automatic cuff devices and can potentially be extended to achieve cuff-less and calibration-free monitoring of BP via widely used smartphones (Chandrasekhar et al., 2018a)(Chandrasekhar et al., 2018b). Fig. 4.1(A) illustrates the oscillometric BP measurement principle. The external pressure of an artery is swept between supra-systolic and sub-diastolic BP levels, and the external pressure is measured and high-pass filtered to yield oscillations indicative of the blood volume. Since the arterial compliance is dependent on transmural pressure (= BP – external pressure), the peak-topeak amplitude of the blood volume oscillations varies with the external pressure. BP is then estimated from the oscillation amplitude versus external pressure function (i.e., "oscillogram") via an algorithm. Fig. 4.1(B) shows popular oscillometric BP estimation algorithms in the literature. The maximum amplitude algorithm estimates mean BP (i.e., the time average of instantaneous BP over the cardiac cycle) as the external pressure at which the oscillogram has peak value (Mauck et al., 1980)(Drzewiecki et al., 1994). The fixed ratio algorithm estimates each of diastolic BP and systolic BP as the external pressure at which the oscillogram is some population-based fraction of its peak value (Drzewiecki et al., 1994)(Geddes et al., 1982). The derivative algorithm estimates diastolic BP and systolic BP as the external pressures at which the oscillogram has maximum and minimum slope, respectively (Drzewiecki & Bronzino, 2006)(Forouzanfar et al., 2015). Note that these algorithms are believed to be related to commercial device algorithms, which are proprietary (Alpert et al., 2014)(Van Montfrans, 2001)(NIH, 2002). The three algorithms are empiricallyinspired rather than theoretically-based. In other words, they may have been conceived with the aid of reference BP measurements rather than first principles. Hence, it is difficult to understand

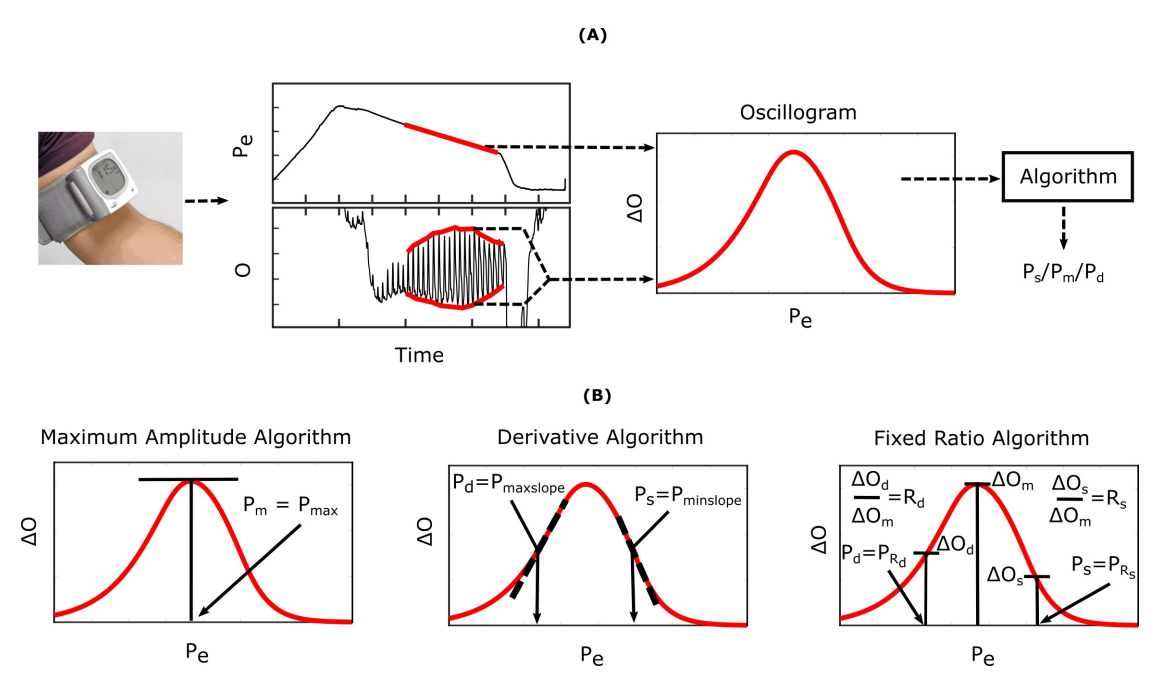


Figure 4.1: Oscillometric blood pressure (BP) measurement principle, which is employed by most automatic cuff devices, and associated algorithms. (A) The external pressure (P_e) of an artery is swept via cuff inflation/deflation, and P_e (i.e., cuff pressure) is measured and high-pass filtered to yield oscillations (O). Systolic BP (P_s) , mean BP (P_m) , and/or diastolic BP (P_d) are then estimated from the oscillogram (peak-to-peak amplitude or envelope difference of the oscillation (ΔO) versus P_e function) via an empirical algorithm. (B) Popular algorithms include the maximum amplitude, derivative, and fixed ratio algorithms (Ng & Small, 1994).

their capabilities and limitations in estimating BP. As a result, the algorithms have previously been examined via mathematical modeling of oscillometry. More specifically, sensitivity analyses were applied to computational oscillometric models to determine the factors that affect the accuracy of the maximum amplitude algorithm (Ramsey, 1979)(Raamat et al., 1999)(Baker et al., 1997)(Ursino & Cristalli, 1996) and fixed ratio algorithm (Drzewiecki et al., 1994)(Ursino & Cristalli, 1996)(Liu et al., 2013)(Raamat et al., 2011). Here, we built upon the past modeling efforts by deriving parametric formulas to explain the popular oscillometric BP estimation algorithms and employing patient data to establish exemplary parameter values and to validate the formulas. The resulting closed-form expressions allow for easier and more complete interpretation of all three popular algorithms while providing new insights that are in contrast to some currently held beliefs about these algorithms.

4.2 The Formulas

To derive formulas to explain the popular oscillometric BP estimation algorithms, we began with a previous mathematical model of the oscillogram, then extended this model, and finally formulated and solved the pertinent equations.

4.2.1 Mathematical Model

The previous oscillogram model (Liu et al., 2017)(Liu et al., 2016) is similar to other such models (Babbs, 2012)(Drzewiecki et al., 1994) and is based on three major assumptions. First, the artery is purely elastic with a sigmoidal blood volume-transmural pressure relationship (V = f(P)). Second, the tissue around the artery is incompressible. Third, the cuff pressure-air volume relation is both static and linear such that the peak-to-peak amplitude of the measured oscillations (Δ O) is proportional to the peak-to-peak amplitude of the arterial blood volume oscillations (Δ V) via a constant k, which reflects the reciprocal of the compliance of the cuff. Fig. 4.2 shows pictorially that these assumptions lead to the following model of the oscillogram:

$$\Delta O = k f(P_s - P_e) - k f(P_d - P_e), \tag{4.1}$$

where P_s and P_d are systolic and diastolic BP, and P_e is the external pressure of the artery.

We built upon this previous model by first differentiating Eq. 4.1 with respect to P_e to yield the following model of the derivative of the oscillogram:

$$\frac{d\delta O}{dP_e} = kg(P_d - P_e) - kg(P_s - P_e),\tag{4.2}$$

where g(.) is the derivative of f(.) and represents the arterial compliance curve. We then conceived a parametric function for g(.) that fits experimental data, leads to closed-form expressions, and has a continuous, first derivative (to facilitate the derivation of some of the expressions) as follows:

$$g(P) = \gamma e^{\frac{P}{\alpha}} \left(-\frac{P}{\alpha} + 1\right) u(-P) + \gamma e^{-\frac{P}{\beta}} \left(\frac{P}{\beta} + 1\right) u(P)$$
(4.3)

where u(.) is the unit-step function, and α , β , and γ are positive-valued parameters. As shown in Fig. 4.3A, α and β reflect the arterial compliance curve widths over negative and positive transmural

pressures, respectively, while γ denotes the height of the curve. Consistent with a sigmoidal blood volume-transmural pressure relation and experimental data (Drzewiecki et al., 1994), 4.3 yields a skewed, unimodal arterial compliance curve that peaks near zero transmural pressure.

Substituting Eq. 4.3 into Eq. 4.2 yields the extended model of the derivative of the oscillogram as follows:

$$\begin{split} \frac{d\Delta O}{dP_e} &= \\ k\gamma e^{\frac{P_d - P_e}{\alpha}} (-\frac{P_d - P_e}{\alpha} + 1)u(-(P_d - P_e)) \\ &+ \\ k\gamma e^{-\frac{P_d - P_e}{\beta}} (\frac{P_d - P_e}{\beta} + 1)u(P_d - P_e) \\ &- \\ k\gamma e^{\frac{P_s - P_e}{\alpha}} (-\frac{P_s - P_e}{\alpha} + 1)u(-(P_s - P_e)) \\ &- \\ k\gamma e^{-\frac{P_s - P_e}{\beta}} (\frac{P_s - P_e}{\beta} + 1)u(P_s - P_e). \end{split}$$

$$\Delta O = k\gamma((P_{d} - P_{e} + 2\beta)e^{-\frac{P_{d} - P_{e}}{\beta}} - (P_{s} - P_{e} + 2\beta)e^{-\frac{P_{s} - P_{e}}{\beta}})$$

$$u(P_{d} - P_{e})$$

$$+ k\gamma(2(\alpha + \beta) + (P_{d} - P_{e} - 2\alpha)e^{\frac{P_{d} - P_{e}}{\alpha}} - (P_{s} - P_{e} + 2\beta)e^{-\frac{P_{s} - P_{e}}{\beta}})$$

$$(u(P_{e} - P_{d}) - u(P_{e} - P_{s}))$$

$$+ k\gamma((P_{d} - P_{e} - 2\alpha)e^{\frac{P_{d} - P_{e}}{\alpha}} - (P_{s} - P_{e} - 2\alpha)e^{\frac{P_{s} - P_{e}}{\alpha}})$$

$$u(P_{e} - P_{s}).$$
(4.5)

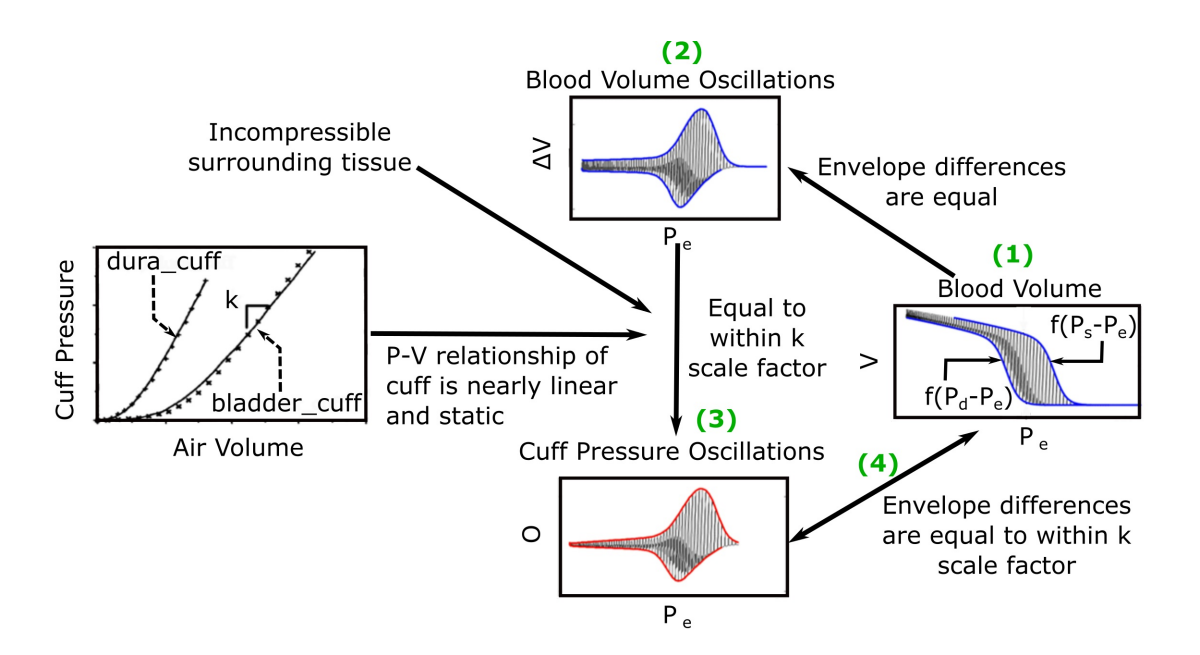


Figure 4.2: **Previous mathematical model of the oscillogram.** (1) The envelope difference of the unmeasured arterial blood volume (V) versus external pressure (P_e) function is equal to the difference in the x-axis reversed blood volume-transmural pressure relationships $(f(P - P_e))$ evaluated at $P = P_s$ and $P = P_d$. (2) This envelope difference is equal to the envelope difference of the blood volume oscillation (ΔV , i.e., high-pass filtered blood volume) versus P_e function. (3) By assuming incompressible tissue around the artery and a linear and static cuff pressure-air volume relation, the latter envelope difference is proportional to the envelope difference of the measured oscillation (O) versus P_e function (i.e., oscillogram) through a k (reciprocal of cuff compliance) scale factor. (The cuff-pressure-air volume relations shown are from two actual cuffs called dura_c uff and bladder_c uff.) (4) The oscillogram may thus be represented as shown in Eq. 4.1

Fig. 4.3(B) illustrates the model predicted derivative of the oscillogram of Eq. 4.4, while Fig. 4.3(C) shows the model predicted oscillogram of Eq. 4.5. These predictions qualitatively correspond to experimental data (see, e.g., Fig. 4.1(A)). However, the extended model does carry a fourth assumption that the arterial compliance curve has a specific shape defined by Eq. 4.3 with maximal value precisely at zero transmural pressure.

4.2.2 Formula for the maximum amplitude algorithm

As shown in Fig. 4.1(B), the maximum amplitude algorithm estimates mean BP (P_m) as the external pressure at which the oscillogram has maximum value (P_{max}). A formula for P_{max} may be found by setting Eq. 4.4 to zero with $P_e = P_{max}$ and invoking $P_d < P_{max} < P_s$ (see Fig. 4.3(B)) as

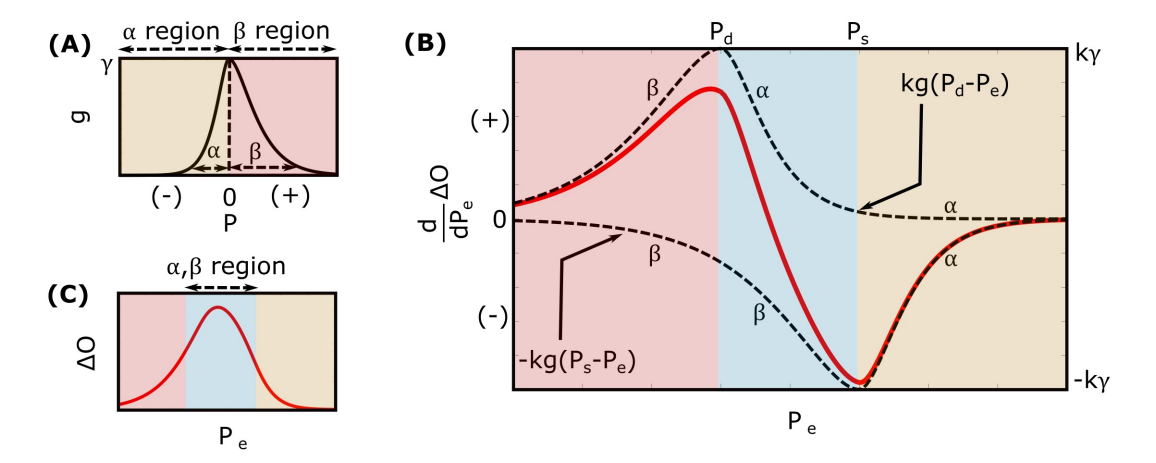


Figure 4.3: **Extended mathematical model of the oscillogram.** (A) Parametric model of the arterial compliance curve as shown in Eq. 4.3) that is physiologic and readily leads to formulas for explaining the oscillometric BP estimation algorithms of Fig. 4.1. The model parameters α and β reflect the compliance curve widths over negative and positive transmural pressures, respectively, while γ denotes the compliance curve height. (B) Model of the derivative of the oscillogram obtained from the derivative of the model shown in Fig. 4.2 and the arterial compliance curve model shown in (A). (C) Model of the oscillogram obtained by integrating the derivative model shown in (B).

follows:

$$k\gamma e^{\frac{P_d - P_{max}}{\alpha}} \left(-\frac{P_d - P_{max}}{\alpha} + 1 \right) = k\gamma e^{-\frac{P_s - P_{max}}{\beta}} \left(\frac{P_s - P_{max}}{\beta} + 1 \right) \tag{4.6}$$

The relevant solution to this equation is readily given as follows:

$$P_{max} = \frac{\alpha}{\alpha + \beta} P_s + \frac{\beta}{\alpha + \beta} P_d \tag{4.7}$$

The final formula of Eq. 4.7 indicates that the maximum amplitude algorithm yields a weighted average of systolic BP and diastolic BP where the weighting is determined by the arterial compliance curve widths.

4.2.3 Formulas for the derivative algorithm

As shown in Fig. 4.1(B), the derivative algorithm estimates diastolic BP and systolic BP as the external pressures at which the oscillogram has maximum slope ($P_{maxslope}$) and minimum slope ($P_{minslope}$), respectively. A formula for $P_{maxslope}$ may be found by employing Eq. 4.4 with

 $P_e = P_{maxslope}$, invoking $P_{maxslope} < P_d$ (see Fig. 4.3(B)), and taking the derivative and setting the equation to zero as follows:

$$\gamma e^{-\frac{P_d - P_{maxslope}}{\beta}} (\frac{P_d - P_{maxslope}}{\beta^2}) = k\gamma e^{\frac{P_s - P_{maxslope}}{\beta}} (\frac{P_s - P_{maxslope}}{\beta^2}). \tag{4.8}$$

The solution to this equation is given as follows:

$$P_{maxslope} = P_d - (\frac{PP}{\frac{PP}{\beta} - 1}) \tag{4.9}$$

where $PP = P_s - P_d$ is the pulse pressure. Using a similar procedure but with $P_{minslope} > P_s$ (see Fig. 4.3(B)), the following formula for $P_{minslope}$ results:

$$P_{minslope} = P_s + (\frac{PP}{e^{\frac{PP}{\alpha}} - 1}) \tag{4.10}$$

The final formulas of Eqs. 4.9 and 4.10 indicate that the derivative algorithm underestimates diastolic BP and overestimates systolic BP by an amount that is dependent on both PP and the arterial compliance curve widths.

4.2.4 Formulas for the fixed ratio algorithm

As shown in Fig. 4.1(B), the fixed ratio algorithm estimates diastolic BP as the external pressure at which the rising portion of the oscillogram is some ratio of its maximal value (P_{R_d} , where R_d is the assumed diastolic ratio) and systolic BP as the external pressure at which the falling portion of the oscillogram is some ratio of its maximal value (P_{R_s}), where R_s is the assumed systolic ratios). Formulas for the true ratios (TR_d and TR_s , i.e., the amplitude of the oscillogram at the actual systolic BP/diastolic BP (e.g., invasive BP values) divided by the maximal oscillogram amplitude) may be derived by substituting P_s or P_d and P_{max} for P_e into Eq. 4.5 as follows:

$$TR_{d} = \frac{\Delta O|_{P_{e}=P_{d}}}{\Delta O|_{P_{e}=P_{max}}} = \frac{2\beta - (PP + 2\beta)e^{-\frac{PP}{\beta}}}{2(\alpha + \beta) - (PP + 2(\alpha + \beta))e^{-\frac{PP}{\alpha + \beta}}}$$
(4.11)

$$TR_{s} = \frac{\Delta O|_{Pe=P_{s}}}{\Delta O|_{Pe=P_{max}}} = \frac{2\alpha - (PP + 2\alpha)e^{-\frac{PP}{\alpha}}}{2(\alpha + \beta) - (PP + 2(\alpha + \beta))e^{-\frac{PP}{\alpha + \beta}}}$$
(4.12)

The final formulas of Eqs. 4.11 and 4.12 indicate that the true ratios vary with PP and the widths of the arterial compliance curve.

To derive formulas for indicating how much error in the presumptive systolic ratio $(R_s - TR_s)$ translates to error in systolic BP $(P_{R_s} - P_s)$, two cases must be considered. One case is an assumed ratio leading to systolic BP underestimation. In this case, the systolic ratio error may be determined from the middle term in Eq. 4.5 along with Eq. 4.12 as follows:

$$R_{S} - TR_{S} = \frac{\Delta O|_{P_{e} = P_{R_{S}}}}{\Delta O|_{P_{e} = P_{max}}} - TR_{S} = \frac{2(\beta) + (P_{d} - P_{R_{S}} - 2\alpha)e^{\frac{P_{d} - P_{R_{S}}}{\alpha}} - (P_{S} - P_{R_{S}} + 2\beta)e^{-\frac{P_{S} - P_{R_{S}}}{\beta}} + (PP + 2\alpha)e^{-\frac{PP}{\alpha}}}{2(\alpha + \beta) - (PP + 2(\alpha + \beta))e^{-\frac{PP}{\alpha + \beta}}}$$
(4.13)

By assuming small systolic BP error $(P_{R_S} \approx P_S)$ and neglecting the terms $e^{\frac{P_d - P_{R_S}}{\alpha}} \approx e^{\frac{PP}{\alpha}}$ (as justified in the Results section), Eq. 4.13 may be linearized as follows:

$$R_{s} - TR_{s} = \frac{2\beta - (P_{s} - P_{R_{s}} + 2\beta)(1 - \frac{P_{s} - P_{R_{s}}}{\beta})}{2(\alpha + \beta) - (PP + 2(\alpha + \beta))e^{-\frac{PP}{\alpha + \beta}}}$$

$$\approx \frac{P_{s} - P_{R_{s}}}{2(\alpha + \beta) - (PP + 2(\alpha + \beta))e^{-\frac{PP}{\alpha + \beta}}}$$

$$(4.14)$$

The other case is an assumed ratio leading to systolic BP overestimation. In this case, the systolic

ratio error may be determined from the last term in Eq. 4.5 along with Eq. 4.12 as follows:

$$R_{S} - TR_{S} =$$

$$\frac{\Delta O|_{P_{e}=P_{R_{S}}}}{\Delta O|_{P_{e}=P_{max}}} - TR_{S} =$$

$$\frac{(P_{d} - P_{R_{S}} - 2\alpha)e^{\frac{P_{d} - P_{R_{S}}}{\alpha}} - (P_{S} - P_{R_{S}} + 2\alpha)e^{\frac{P_{S} - P_{R_{S}}}{\beta}} - 2\alpha + (PP + 2\alpha)e^{-\frac{PP}{\alpha}}}{2(\alpha + \beta) - (PP + 2(\alpha + \beta))e^{-\frac{PP}{\alpha + \beta}}}$$

$$(4.15)$$

By likewise simplifying Eq. 4.15, the identical equation on the right-hand-side of Eq. 4.14 results. Solving for P_{R_S} in this common equation thus yields the following small error formula:

$$P_{R_S} \approx P_S - (2(\alpha + \beta) - (PP + 2(\alpha + \beta))e^{-\frac{PP}{\alpha + \beta}})(R_S - TR_S)$$
(4.16)

An analogous formula for translating diastolic ratio error to small diastolic BP error may be derived using a similar procedure but neglecting terms $e^{-\frac{P_S-P_{R_d}}{\beta}} \approx e^{-\frac{PP}{\beta}}$ and is given as follows:

$$P_{R_d} \approx P_d + (2(\alpha + \beta) - (PP + 2(\alpha + \beta))e^{-\frac{PP}{\alpha + \beta}})(R_d - TR_d)$$
(4.17)

The final small error formulas of Eqs. 4.16 and 4.17 indicate that error in the presumptive ratios maps to error in BP by a scale factor determined by PP and the arterial compliance curve widths.

4.3 Results

We provide results to first demonstrate the validity of the mathematical model and provide exemplary parameter estimates and to then validate the formulas themselves.

4.3.1 Mathematical model and parameter estimates

The mathematical model of Eq. 4.5 was able to fit the oscillograms with a normalized-root-mean-squared-error (NRMSE) of $8.5\pm0.5\%$ (mean \pm SE). Fig. 4.4(A) illustrates the resulting model parameter estimates. The β estimates were larger than the α estimates (13.8 \pm 0.7 versus 11.4 \pm 0.9 mmHg; p = 0.03), which is consistent with the expected right-skewed compliance curve (Drzewiecki

et al., 1994). The β estimates also increased after nitroglycerin administration (15.4±1.2 versus 12.8±0.9 mmHg; p = 0.007), which is consistent with the expected drug-induced increase in arterial compliance over the physiologic positive transmural BP regime, while the α estimates did not change following the intervention (11.7±1.6 versus 10.8±1.2 mmHg; p = NS).

4.3.2 Formula for the maximum amplitude algorithm

The maximum amplitude algorithm detects the external pressure at which the oscillogram peaks (P_{max}) , which has commonly been believed to denote mean BP. However, the formula of Eq. 4.7 predicts that P_{max} is instead a weighted average of systolic BP and diastolic BP. Fig. 4.5(left) shows correlation and Bland-Altman plots of P_{max} predicted by the formula versus P_{max} measured via the maximum amplitude algorithm. For comparison, Fig. 4.5 (right) likewise shows invasive mean BP (P_m) versus measured P_{max} . As can be seen, the formula predicted P_{max} well and clearly better than P_m , especially at higher pressures.

4.3.3 Formula for the derivative algorithm

The derivative algorithm detects the external pressures at which the oscillogram has maximum slope $(P_{maxslope})$ to estimate diastolic BP and minimum slope $(P_{minslope})$ to estimate systolic BP. The formulas of Eqs. 4.9 and (4.10 predict that the BP errors of the derivative algorithm are $(\frac{PP}{\frac{PP}{e}})$ for diastolic BP and $(\frac{PP}{\frac{PP}{e}})$ for systolic BP. Fig. 4.4(B) shows histograms of the estimated $(\frac{PP}{\frac{PP}{e}})$ and $(\frac{PP}{\frac{PP}{e}})$. Since these errors are small (0.9±0.4 or 1.4±0.4 mmHg), the formulas predict that the derivative algorithm should yield accurate BP estimates. Fig. 4.6(A) shows correlation and Bland-Altman plots of $P_{maxslope}$ and $P_{minslope}$ measured via the derivative algorithm versus invasive diastolic BP (P_d) and invasive systolic BP (P_s) . As can be seen, the bias errors (mean of the errors) are small, which is consistent with the formula predictions. However, the precision errors (standard deviation of the errors) are appreciable. The reason is surely due to derivative-induced amplification of oscillogram noise, which is common and often of high

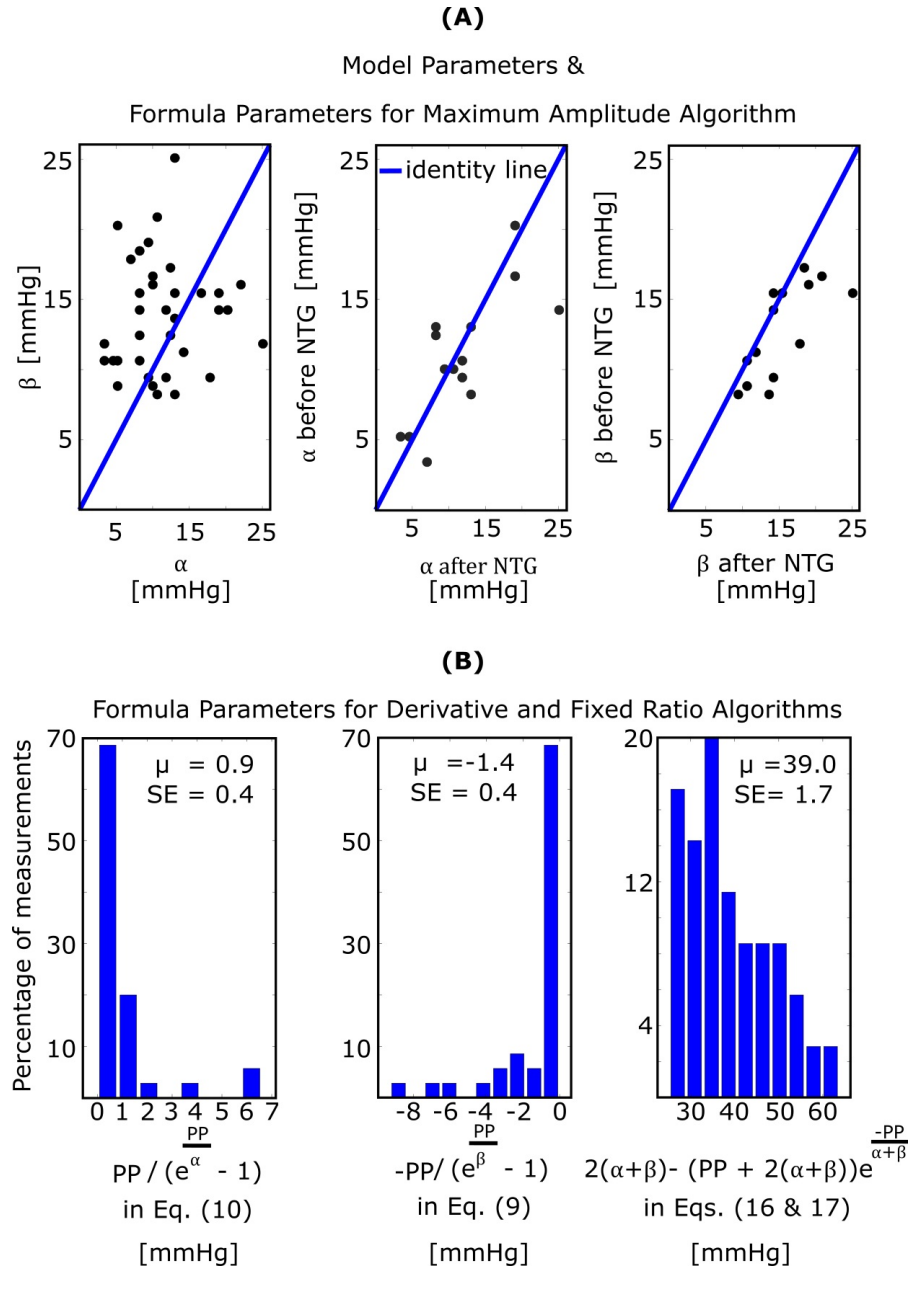


Figure 4.4: Model and formula parameter values obtained by fitting the model to measured oscillograms from patients. (A) Model parameters and formula parameters for the maximum amplitude algorithm (see Eq. 4.7). The parameters α and β again reflect the arterial compliance curve widths over negative and positive transmural pressures, respectively (see Fig 4.3(A)). (B) Formula parameters for the derivative and fixed ratio algorithms. The two histograms on the left show the values of the BP errors in the formulas for the derivative algorithm (see Eqs. 4.9 and 4.10), while the histogram on the right shows the values of the scale factor mapping ratio error to small BP error in the formulas for the fixed ratio algorithm (see Eqs. 4.16 and 4.17). PP is pulse pressure; μ , mean value; SE, standard error.

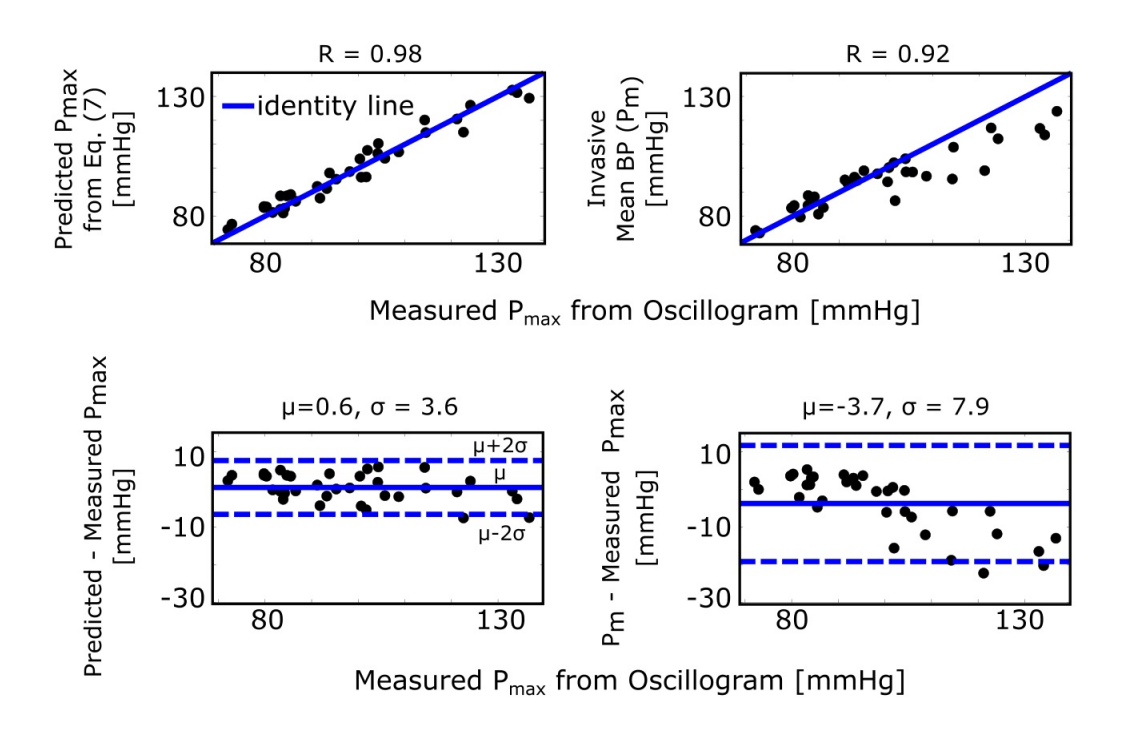


Figure 4.5: Validation results for the formula for explaining the maximum amplitude algorithm. Correlation and Bland-Altman plots of P_{max} (external pressure at which the oscillogram peaks) predicted by the formula versus P_{max} measured from the oscillogram via the maximum amplitude algorithm (left plots) and of invasive mean BP (P_m) versus measured P_{max} (right plots). R is the correlation coefficient; μ , mean of the errors (bias error); and σ , standard deviation of the errors (precision error).

frequency character (due to, e.g., respiration, heart rate variability, and motion) but not considered by the formulas. Fig. 4.6(B) illustrates a representative example of the impact of noise in the patient data on the derivative of the oscillogram before any filtering.

4.3.4 Formulas for the fixed ratio algorithm

The fixed ratio algorithm detects the external pressures at which the descending portion of the oscillogram is some assumed constant ratio of its maximal amplitude (P_{R_s}) to estimate systolic BP and at which the ascending portion of the oscillogram is some assumed constant ratio of it maximal amplitude (P_{R_d}) to estimate diastolic BP. The true systolic and diastolic ratios (T_s and T_d) in the formulas of Eqs. 4.11 and 4.12 are defined as the ratios at which these externals pressures

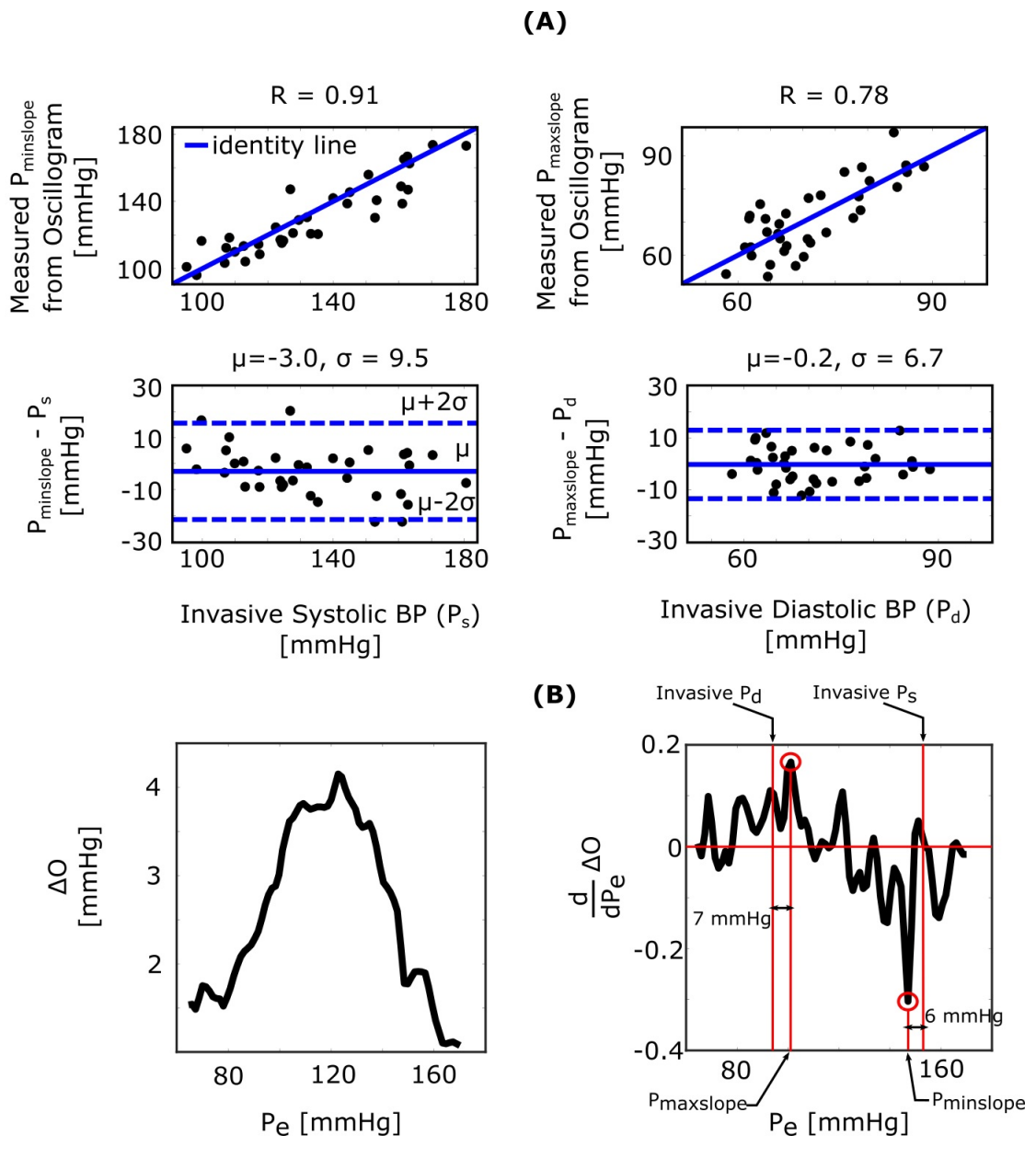


Figure 4.6: Validation results for the formulas for explaining the derivative algorithm. (A) Correlation and Bland-Altman plots of $P_{maxslope}$ and $P_{minslope}$ (external pressures at which the oscillogram has maximal and minimal slopes) measured from the oscillogram via the derivative algorithm versus invasive diastolic BP (P_d) and invasive systolic BP (P_s) . Consistent with the formula predictions, the bias errors are small. The appreciable precision errors are due to measurement noise, which is not considered by the formulas. (B) A representative oscillogram (before any filtering or model fitting) and its derivative illustrating the impact of typical high frequency measurement noise (due to, e.g., respiration, heart rate variability, and motion) on the correspondence between the detected $P_{minslope}/P_{maxslope}$ and P_s/P_d .

correspond to the actual BP levels. Fig. 4.7(A) shows correlation and Bland-Altman plots of TR_s and TR_d predicted by the formulas of Eqs. 4.11 and 4.12 versus TR_s and TR_d measured by evaluating the oscillogram at invasive systolic BP and diastolic BP. As can be seen, these formulas were generally able to predict the true ratios, which varied widely (over a 0.5-0.6 range). $P_{R_s} - P_s$ and P_{R_d} – P_d in the formulas of Eqs. 4.16 and 4.17 respectively represent the systolic BP and diastolic BP errors of the fixed ratio algorithm. Fig. 4.7(B) shows analogous plots of $P_{R_s} - P_s$ and P_{R_J} – P_d predicted by the small error formulas of Eqs. 4.16 and 4.17 versus P_{R_S} – P_S and P_{R_d} – P_d measured as the difference between the BP estimates of the fixed ratio algorithm (with ratios given by the average of the measured TR_s and TR_d over all patients) and the invasive BP values. Note that these formulas neglected $e^{-\frac{PP}{\alpha}}$, $e^{-\frac{PP}{\beta}}$, which is now justified by the small BP error terms of the formulas for the derivative algorithm (see Fig. 4.4(B)). As can be seen, the formulas of Eqs. 4.16 and 4.17 were able to predict small BP errors but, as expected, became less accurate with increasing errors. Fig. 4.4(B) additionally shows the histogram of the estimated $2(\alpha + \beta) - (PP + 2(\alpha + \beta))e^{-\frac{PP}{\alpha + \beta}}$ (the scale factor mapping ratio error to BP error) in the formulas of Eqs. 4.16 and 4.17. These estimates indicate that a ratio error of 0.2 (e.g., the assumed ratio is 0.5 but the true ratio is 0.7) would yield about an 8 mmHg BP error (39.0 \pm 1.7 times 0.2).

4.4 Discussion

This study is generally about mathematical modeling of the oscillometric BP measurement principle. While recent studies have employed such modeling towards improving oscillometric BP estimation accuracy (Babbs, 2012)(Liu et al., 2017)(Liu et al., 2016), the purpose of this study was to establish parametric formulas with exemplary parameter values to explain three popular empirical algorithms in the literature for oscillometric BP estimation: (1) maximum amplitude, (2) derivative, and (3) fixed ratio algorithms (Fig. 1). To derive the closed-form expressions, we extended a previous mathematical model of the oscillogram (Figs. 4.2 and 4.3) and then employed the extended model to formulate and solve the pertinent equations. To determine the formula parameter values, we fitted the model to oscillograms measured from patients covering a wide BP

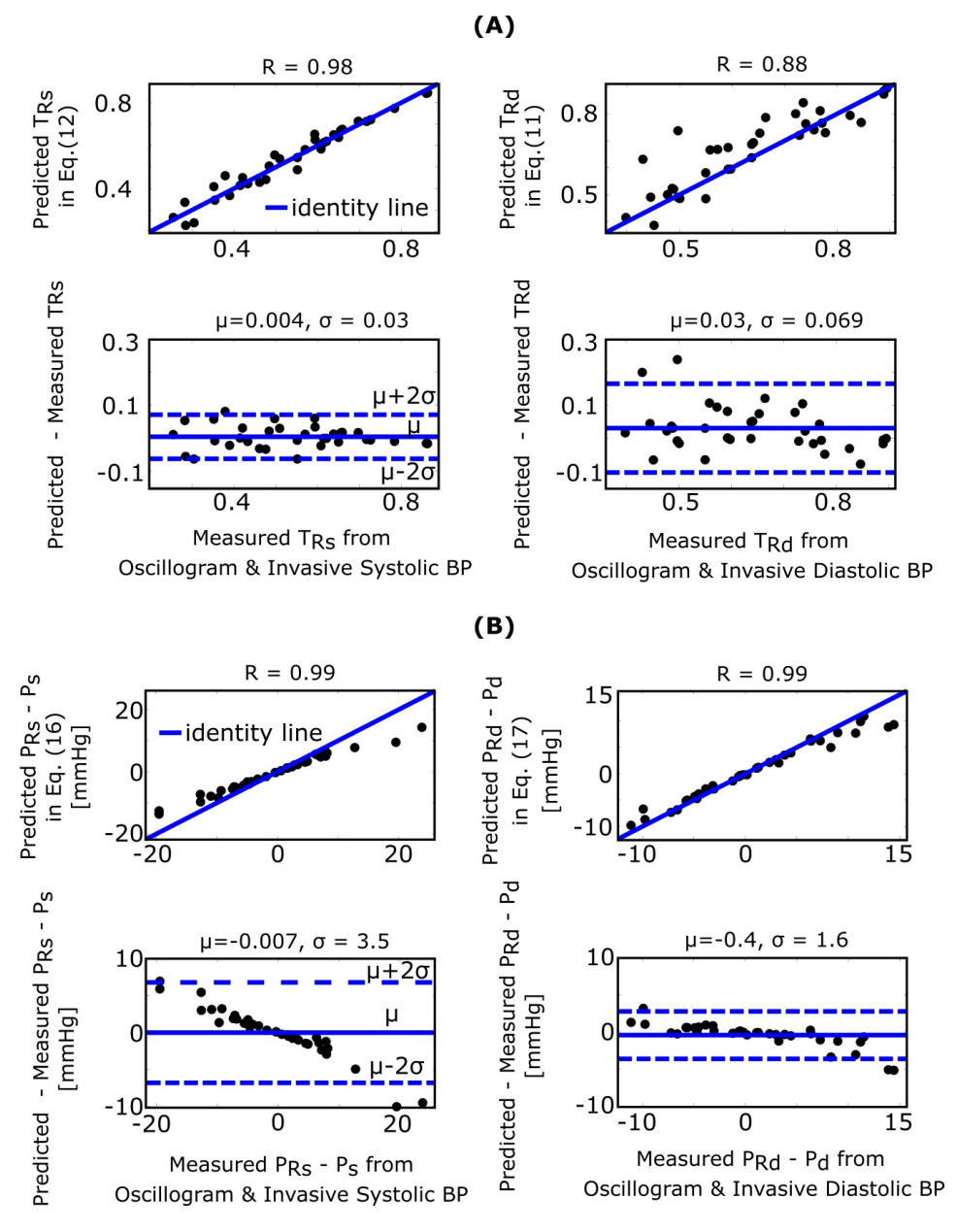


Figure 4.7: **Validation results for the formulas for explaining the fixed ratio algorithm.** (A) Correlation and Bland-Altman plots of TR_s and TR_d (true systolic and diastolic ratios, i.e., the ratios of the oscillogram evaluated at the actual BP levels) predicted by the formulas of Eqs. 4.11 and 4.12 versus TR_s and TR_d measured by evaluating the oscillogram at invasive systolic BP and diastolic BP. (B) Analogous plots of $P_{R_s} - P_s$ and $P_{R_d} - P_d$ (BP errors of fixed ratio algorithm) predicted by the small error formulas of Eqs. 4.16 and 4.17 versus $P_{R_s} - P_s$ and $P_{R_d} - P_d$ measured as the difference between the BP estimates via application of the fixed ratio algorithm (with ratios given by the average of the measured TR_s and TR_d over all the patients) to the oscillogram and the invasive BP values.

range (Fig. 4.4). A key step was to define a parametric function to represent the arterial compliance curve in the model (Eq. 4.2) that is able to fit experimental data while leading to analytical solutions. We also sought a function that has a continuous, first derivative to readily arrive at the solutions. To satisfy these desired attributes, we conceived the function of Eq. 4.3 (Fig. 4.3(A)) and showed that the model with this function (Eq. 4.5) can fit the measured oscillograms $(8.5\pm0.5\% \text{ error})$. Other parametric functions to define the arterial compliance curve include an asymmetric exponential function (Babbs, 2012)(Baker et al., 1997) and an asymmetric normal function as shown Eq. 4.18 and 4.19.

Eq. 4.18 can lead to closed-form expressions. However, its first derivative is discontinuous, so the derivation is not as clean. More importantly, Eq. 4.18 does not allow for better fitting of the measured oscillograms $(9.3\pm0.5\% \text{ vs. } 8.5\pm0.5\% \text{ error}; p = 4.8x10^{-4} \text{ via paired t-test after log transformation of the data})$. While this quantitative difference in the fitting error may not seem large, the fitting difference can be seen visually through plots of model-predicted versus measured oscillograms. Eq. 4.19 does allow for better oscillogram fitting $(7.7\pm0.4\% \text{ vs. } 8.5\pm0.5\% \text{ error}; p = 0.001)$. However, this equation does not lead to closed-form expressions, because, for example, the integral of a Gaussian cannot be solved analytically.

While we have not proven that Eq. \pm is the optimal parametric arterial compliance curve function in terms of best data fitting while yielding closed-form expressions, we did demonstrate the validity of the resulting formulas by showing that they can predict experimental data (Figs. 4.5-4.7). Note that these results also substantiate the secondary assumption of Eq. 4.3 that the arterial compliance curve peaks at zero transmural pressure. For example, Fig. 4.5 shows that the formula of Eq. 4.7 predicts P_{max} detected by the maximum amplitude algorithm with little bias (0.6 mmHg). If the peak of the compliance curve were instead at an average of γ mmHg, then the bias would have been $-\gamma$ mmHg. Fig. 4.8 consolidates and summarizes all of the established formulas. We interpret and discuss these formulas in the following. The formula for the maximum amplitude algorithm indicates that the algorithm actually estimates a weighted average of systolic BP and diastolic BP (0.45 and 0.55 weighting here) in contrast to the commonly held belief that

it yields an estimate of mean BP (compare left plots with right plots in Fig. 4.5) (Mauck et al., 1980)(Drzewiecki et al., 1994). An interesting coincidence is that a popular estimate of mean BP is obtained from systolic BP and diastolic BP as $P_m = 0.4P_s + 0.6P_d$ (Bos et al., 2007). Since this estimate is imperfect and generally becomes less accurate with increasing pressure, it does not conflict with the new finding here that the maximum amplitude algorithm does not estimate mean BP. We also mention that, for this particular algorithm, the parametric arterial compliance curve functions of Eq. 4.18 or 4.19 do lead to analytical formulas that likewise indicate that the algorithm yields a weighted average of systolic BP and diastolic BP instead of mean BP.

The formulas for the derivative algorithm (Fig. 4.8) predict that the algorithm will overestimate systolic BP and underestimate diastolic BP but only by a small amount (< 1.5 mmHg here), as PP is often substantially larger than the arterial compliance curve widths such that the two compliance curves in the model (Eq. 4.2) are well separated (Fig. 4.3(B)). We also mention that the parametric arterial compliance curve of Eq. 4.18 indicates that the derivative algorithm yields systolic BP and diastolic BP without any error (Babbs, 2012). This prediction is in contrast to a previous study indicating that the algorithm appreciably overestimates auscultation systolic BP (+9% bias error) and underestimates auscultation diastolic BP (-6% bias error) (Drzewiecki & Bronzino, 2006). These larger BP bias errors may be explained to a significant extent by the fact that auscultation underestimates systolic BP and overestimates diastolic BP (ISO, 2013). However, the formulas do not consider measurement noise. Since differentiation amplifies noise, common high frequency oscillogram measurement artifact due to, for example, respiration, heart rate variability, and motion is a major factor that can introduce appreciable BP precision errors in practice (Fig. 4.6) (Babbs, 2012). Hence, the formulas suggest that if a robust algorithm for faithfully detecting the maximum and minimum slopes could be developed, the accuracy of oscillometric BP measurement could be significantly enhanced. The first two formulas for the fixed ratio algorithm (Fig. 4.8) indicate that the true systolic and diastolic ratios vary with the arterial compliance curve widths and PP and thus considerably (0.5-0.6 in Fig. 4.7(A)). This prediction is consistent with those of previous computational sensitivity analysis and modeling studies of the fixed ratio algorithm

(Babbs, 2012)(Drzewiecki et al., 1994)(Ursino & Cristalli, 1996)(Liu et al., 2013)(Raamat et al., 2011). However, these earlier studies only provided qualitative rather than exact relationships. The true ratio formulas here may be examined to glean further insight. By taking the derivative with respect to each of the three parameters (α, β, PP) , it can be deduced that the numerator and denominator of the true ratio formulas (which are the same functions but with different parameter values) increase as each parameter increases and then plateau with further parameter increases. It can then be inferred that the true systolic ratio increases with increasing α and decreases with increasing β and PP, while the true diastolic ratio increases with increasing β and decreases with increasing α and PP. The last two formulas for the fixed ratio algorithm (Fig. 4.8) indicate that error in the presumptive ratios translates to significant BP errors (e.g., a ratio error of 0.2 leads to an 8 mmHg BP error here). Note that the scale factor that maps ratio error to BP error is identical to the denominator of the true ratio formulas (Fig. 4.8). Hence, the scale factor increases with α, β , or PP. Similarly, this prediction is consistent with and builds upon the previous computational sensitivity analysis studies (Drzewiecki et al., 1994)(Ursino & Cristalli, 1996)(Liu et al., 2013)(Raamat et al., 2011). However, these formulas are only valid for small errors, and larger ratio errors may be amplified even more to yield very large BP errors (Fig. 4.7(B)). In sum, the fixed ratio algorithm may be generally inaccurate.

4.5 Materials and methods

To determine the parameter values and demonstrate the validity of the mathematical model and formulas, we analyzed patient data.

4.5.1 Patient Data

We leveraged previously collected, de-identified patient data. These data are described in detail elsewhere (Cheng et al., 2013)(Cheng et al., 2012). Briefly, we started with data typically comprising two consecutive oscillometric cuff pressure waveforms via repeated inflation/deflation cycles of an upper arm cuff device (WatchBP Office, Microlife AG, Switzerland) and a reference brachial BP

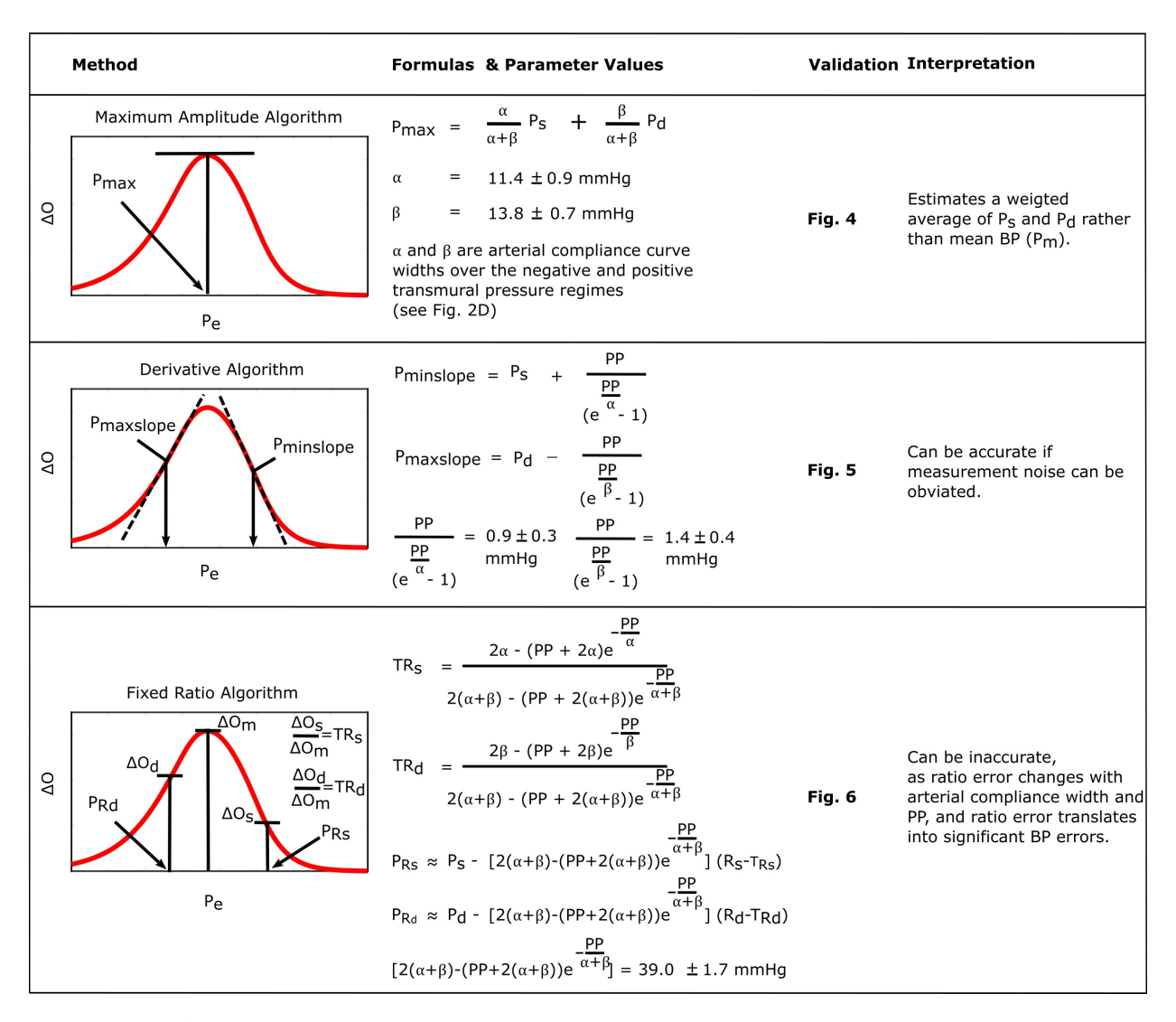


Figure 4.8: Summary of the established formulas for explaining popular oscillometric BP estimation algorithms.

waveform via an intra-arterial catheter in the opposite arm from 33 cardiac catheterization patients before and after sublingual nitroglycerin administration. We excluded data based on three criteria: (1) invasive diastolic BP < the minimum Microlife device cuff pressure of 60 mmHg or invasive systolic BP > the maximum Microlife device cuff pressure (to preclude inaccurate detection of the maximum and minimum slopes of the oscillogram); (2) obvious artifact in the oscillometric cuff pressure waveforms (which is not accounted for by the formulas) or unsteady brachial BP waveforms (to preclude unreliable reference measurements) as ascertained by visual inspection; or (3) inter-arm cuff BP differences > 10 mmHg (to likewise preclude unreliable reference measurements).

A total of 28 baseline and 26 nitroglycerin measurement sets from 21 patients (age of 64 ± 14 years; 80% male; BMI of 27.2 ± 4.8 kg/m2; 24% diabetic; and 63% hypertensive) remained for analysis. The 54 total measurement sets comprised two measurement sets before nitroglycerin in 11 subjects and after nitroglycerin in eight subjects as well as one measurement set before nitroglycerin in six subjects and after nitroglycerin in ten subjects. Fourteen of the subjects had measurement sets both before and after nitroglycerin. The data notably covered a wide BP range (95-180 mmHg for reference systolic BP and 58-88 mmHg for reference diastolic BP).

4.5.2 Data analysis

We first constructed the oscillogram from the measured oscillometric cuff pressure waveforms. Our procedure was similar to that described elsewhere (Liu et al., 2016). Briefly, we (1) band-pass filtered the measured waveforms to extract the cuff pressure oscillations; (2) detected the maxima and minima of the oscillations; (3) filtered these extrema as a function of cuff pressure with a 10-mmHg rectangular window; (4) linearly interpolated the discrete data; and (4) subtracted the so-obtained upper and lower envelopes to yield the oscillogram.

We then analyzed the oscillograms to assess the validity of the model and to determine exemplary formula parameter values. In particular, we set P_s and P_d in Eq. 4.5 to the average invasive systolic BP and diastolic BP during the time period of the oscillogram and set $k\gamma$ in the equation so as to equate the peak values of the model predicted and measured oscillograms. We then estimated the two remaining free parameters, α and β , by (1) varying the parameters over a physiologic range $(0 < \alpha, \beta < 30)$; (2) computing the mean squared error between the model predicted oscillogram and the middle of the measured oscillogram (i.e., the oscillogram over the "foot-to-foot" cuff pressure range, wherein foot is defined analogously to the onset of a BP pulse) for each candidate pair of parameters; and (3) identifying the parameter pair that yielded the minimum mean squared error. We evaluated the model in terms of the root-mean-square of the fitting error between the model predicted and measured oscillograms normalized by the root-mean-square of the measured oscillogram as well as comparisons of the average α and β estimates using paired t-tests and

expectations based on known physiology.

We finally analyzed the oscillograms to assess the validity of the formulas themselves. More specifically, we applied the popular algorithms to estimate BP from the oscillograms. To mitigate noise, especially when applying the derivative algorithm, we first fitted an asymmetric normal function similar to Eq. 4.19, but with a non-zero mean value, to the middle of the oscillogram using the MATLAB fmincon function (interior-point algorithm). To establish the fixed ratio values, we computed the ratios at the invasive systolic BP and diastolic BP for each oscillogram and then averaged the ratios. We then assessed the formula predictions, with α and β set to their estimated values and P_s and P_d set to their invasive BP values, against the algorithm estimates in terms of a correlation plot and Bland-Altman plot (difference in the predicted and measured values versus the accurate measured values rather than the average of the two values). Note that whenever repeated oscillometric cuff pressure waveforms were available, we averaged the pair of results.

$$g_{exp} = \gamma_{exp} e^{\frac{P}{\alpha_{exp}}} u(-P) \gamma_{exp} e^{\frac{-P}{\beta_{exp}}} u(P)$$
(4.18)

$$g_{norm} = \gamma_{norm} e^{-\frac{P}{\alpha exp}^2} u(-P) \gamma_{norm} e^{-\frac{P}{\beta exp}^2} u(P)$$
 (4.19)

4.6 Conclusion

In conclusion, oscillometry is the BP measurement principle of most automatic cuff devices and has thus been a workhorse in hypertension management. This principle may also be emerging as a means for achieving cuff-less and calibration-free BP monitoring via smartphones (Chandrasekhar et al., 2018a)(Chandrasekhar et al., 2018b) and may thus improve hypertension awareness and control rates. Oscillometric devices estimate BP from the measured oscillogram via an empirical algorithm. In this study, we explained perhaps the three most popular empirical algorithms in the literature (Ng & Small, 1994) through formulas. We specifically derived formulas based on a mathematical model of the oscillogram, determined exemplary formula parameter values by fitting

the model to patient oscillograms, and validated the model and formulas using patient data. The resulting formulas are not merely confirmatory of present knowledge and past studies. In fact, the formula for the maximum amplitude algorithm indicates that the algorithm estimates a weighted average of systolic BP and diastolic BP rather than the commonly held belief that it estimates mean BP. Furthermore, the formulas for the derivative algorithm indicate that the algorithm can estimate systolic BP and diastolic BP with small bias errors, which is in contrast to a previous study indicating that it appreciably overestimates systolic BP and underestimates diastolic BP (Drzewiecki & Bronzino, 2006). The formulas for the fixed ratio algorithm add to previous modeling studies by indicating the precise dependency of the true ratios on arterial properties and the precise mapping of small ratio errors to small BP errors. In these ways, this study facilitates understanding of the capabilities and limitations of the important algorithms in estimating BP. The study may also be of some value towards improving algorithm accuracy, which has been called for in recent clinical publications (Muntner et al., 2019)(Picone et al., 2017). For example, an optimization algorithm to fit the oscillogram model to the measured oscillogram (see (Babbs, 2012)(Li et al., 2017)(Liu et al., 2016)) may more accurately estimate BP. Alternatively, a simpler algorithm to faithfully identify the maximum and minimum oscillogram slopes in the presence of noise could allow the derivative algorithm to achieve low precision error.

CHAPTER 5

FUTURE WORK

This thesis discuss a new method to measure blood pressure via the finger pressing oscillometry. To test this approach, we developed a smartphone based device and an iPhone application. In future, we may use thin film sensors on top of the smartphone phone (see Fig. 5.1 5.2) to make the device user friendly.

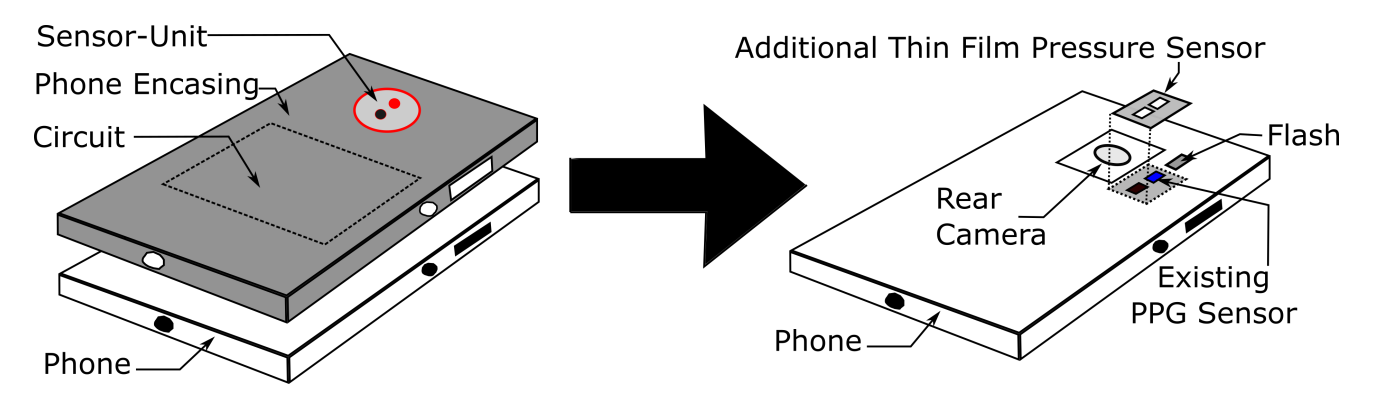


Figure 5.1: Future version(1) of the smartphone based BP monitoring device.

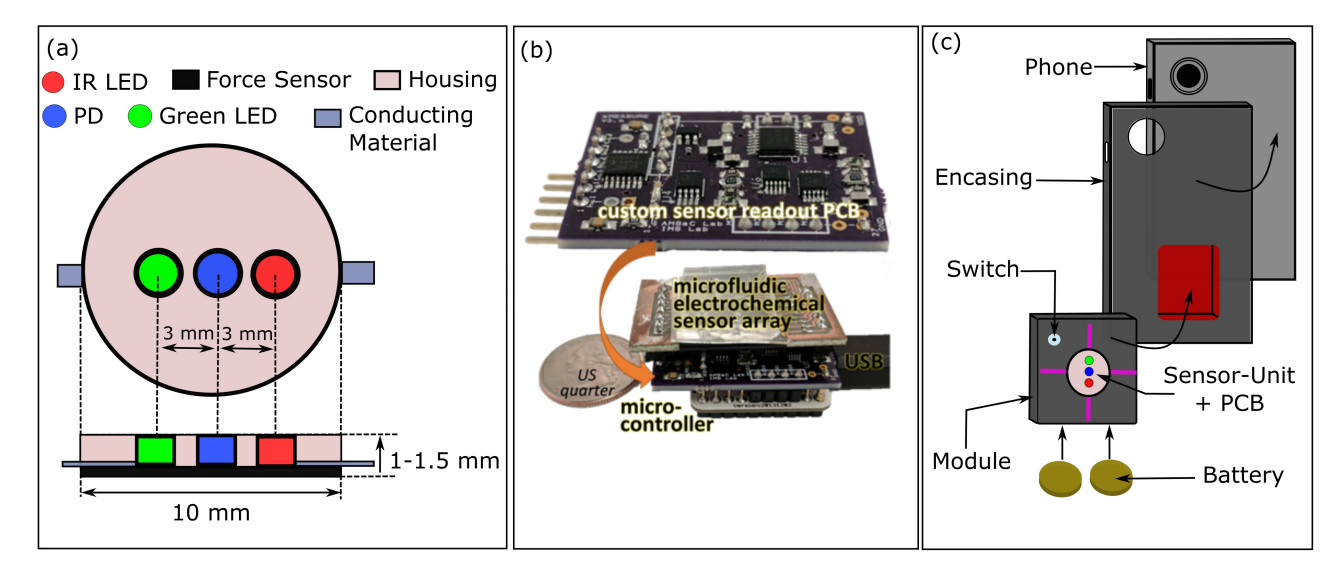


Figure 5.2: Future version (2) of the smartphone based BP monitoring device.

BIBLIOGRAPHY

BIBLIOGRAPHY

- Agarwal, Rajiv, Jennifer E. Bills, Tyler J.W. Hecht & Robert P. Light. 2011. Role of home blood pressure monitoring in overcoming therapeutic inertia and improving hypertension control: A systematic review and meta-analysis. *Hypertension* 57(1). 29–38.
- Alpert, Bruce S., David Quinn & David Gallick. 2014. Oscillometric blood pressure: A review for clinicians. *Journal of the American Society of Hypertension* 8(12). 930–938.
- Apple. 2018. Ui kit. https://developer.apple.com/documentation/UIKit.
- Babbs, Charles F. 2012. Oscillometric measurement of systolic and diastolic blood pressures validated in a physiologic mathematical model. *Biomedical Engineering Online* 11(56). 1–22.
- Baker, P. D., D. R. Westenskow & K. Kück. 1997. Theoretical analysis of non-invasive oscillometric maximum amplitude algorithm for estimating mean blood pressure. *Medical and Biological Engineering and Computing* 35(3). 271–278.
- Bastawrous, Andrew & Matthew J. Armstrong. 2013. Mobile health use in low-and high-income countries: An overview of the peer-reviewed literature. *Journal of the Royal Society of Medicine* 106(4). 130–142.
- Beulen, Bart W A M M, Nathalie Bijnens, Gregory G Koutsouridis, Peter J Brands, Marcel C M Rutten & Frans N van de Vosse. 2011. Toward Noninvasive Blood Pressure Assessment in Arteries by Using Ultrasound. *Ultrasound in Medicine and Biology* 37(5). 788–797.
- Bos, Willem J.W. JW, Elisabeth Verrij, Hieronymus H. Vincent, Berend E. Westerhof, Gianfranco Parati & Gert A. van Montfrans. 2007. How to assess mean blood pressure properly at the brachial artery level. *Journal of Hypertension* 25(4). 751–755.
- Chamary, JV. 2017. 3d touch in iphone 6s isn't just a gimmick. here's how it works. https://www.forbes.com/sites/jvchamary/2015/09/12/3d-touch-iphone-6s/#2c8ef9764cee.
- Chandrasekhar, Anand, CS. Kim, Mohammed Naji, Keerthana Natarajan, JO. Hahn & Ramakrishna Mukkamala. 2018a. Smartphone-based blood pressure monitoring via the oscillometric finger pressing method. *Science Translational Medicine* 10(431). eaap8674.
- Chandrasekhar, Anand, Keerthana Natarajan, Mohammad Yavarimanesh & Ramakrishna Mukkamala. 2018b. An iphone application for blood pressure monitoring via the oscillometric finger pressing method. *Scientific Reports* 8(1). 18–23.
- Cheng, Hao Min, Shih Hsien Sung, Yuan Ta Shih, Shao Yuan Chuang, Wen Chung Yu & Chen Huan Chen. 2013. Measurement accuracy of a stand-alone oscillometric central blood pressure monitor: A validation report for microlife WatchBP office central. *American Journal of Hypertension* 26(1). 42–50.

- Cheng, Hao-min Min, Shih-hsien Hsien Sung, Yuan-ta Ta Shih, Shao-yuan Yuan Chuang, Wenchung Chung Yu & Chen-huan Huan Chen. 2012. Measurement of Central Aortic Pulse Pressure: Noninvasive Brachial Cuff-Based Estimation by a Transfer Function Vs. a Novel Pulse Wave Analysis Method. *American Journal of Hypertension* 25(11). 18–20.
- Curtin, Melanie. 2018. Are you on your phone too much? the average person spends this many hours on it every day. https://www.inc.com/melanie-curtin/.
- Daniil. 2015. Huawei mate s force touch demo [english]. https://www.youtube.com/watch?v=ta6be0vyhYE.
- Drzewiecki, Garry & Joseph D. Bronzino. 2006. Noninvasive Arterial Blood Pressure and Mechanics. In Joseph D. Bronzino (ed.), *The biomedical engineering handbook. medical devices and systems*, chap. 55, 55–7, 55–8. Taylor & Francis Group 3rd edn.
- Drzewiecki, Garry., R. Hood & H. Apple. 1994. Theory of the oscillometric maximum and the systolic and diastolic detection ratios. *Annals of Biomedical Engineering* 22(1). 88–96.
- FMS. 2012. The finapres nova has received 510(k) clearance from the us fda! http://www.finapres.com/.
- Forouzanfar, Mohamad, Hilmi R. Dajani, Voicu Z. Groza, Miodrag Bolic, Sreeraman Rajan & Izmail Batkin. 2015. Oscillometric blood pressure estimation: Past, present, and future. *IEEE Reviews in Biomedical Engineering* 8. 44–63.
- Geddes, L. A., M. Voelz, C. Combs, D. Reiner & C. F. Babbs. 1982. Characterization of the oscillometric method for measuring indirect blood pressure. *Annals of Biomedical Engineering* 10(6). 271–280. doi:10.1007/BF02367308.
- Gizdulich, Paolo, Andriana Prentza & Karel H. Wesseling. 1997. Models of brachial to finger pulse wave distortion and pressure decrement. *Cardiovascular Research* 33(3). 698–705.
- Hansen, S. & M. Staber. 2006. Oscillometric blood pressure measurement used for calibration of the arterial tonometry method contributes significantly to error. *European Journal of Anaesthesiology* 23(9). 781–787.
- Ibrahim, M Mohsen & Albertino A. Damasceno. 2012. Hypertension in developing countries. *Lancet* 380. 611–619.
- Imholz, B P, W Wieling, G A Van Montfrans & K H Wesseling. 1998. Fifteen years experience with finger arterial pressure monitoring: assessment of the technology. *Cardiovascular research* 38(3). 605–616.
- ISO. 2013. Non-invasive sphygmomanometers—part 2: Clinical investigation of automated measurement type. https://www.iso.org/standard/57977.html.
- Lemay, M., M. Bertschi, J. Sola, P. Renevey, J. Parak & I. Korhonen. 2014. Application of Optical Heart Rate Monitoring. In Michael R. Neuman & Edward Sazonov (eds.), *Wearable sensors: Fundamentals, implementation and applications*, 105–130. Elsevier.

- Lewington, S., R. Clarke, N. Qizilbash, R. Peto, R. Collins & Collaboration Prospective studies. 2002. Age-specific relevance of usual blood pressure to vascular mortality: a meta-analysis of individual data for one million adults in 61 prospective studies. *Lancet* 360. 1903–1913.
- Li, Ye, Haotian Gu, Henry Fok, Jordi Alastruey & Philip Chowienczyk. 2017. Forward and Backward Pressure Waveform Morphology in Hypertension. *Hypertension* 69(2). 375–381.
- Liu, Jiankun, Hao-min Cheng, Chen-huan Chen, Shih-hsien Sung, Jin-oh Hahn & Ramakrishna Mukkamala. 2017. Patient-Specific Oscillometric Blood Pressure Measurement: Validation for Accuracy and Repeatability. *IEEE Journal of Translational Engineering in Health and Medicine* 5. 1–10.
- Liu, Jiankun, Hao-min Cheng, Chen-huan Chen, Shih-hsien Sung, Mohsen Moslehpour, Jin-oh Hahn & Ramakrishna Mukkamala. 2016. Patient-specific oscillometric blood pressure measurement. *IEEE Transactions on Biomedical Engineering* 63(6). 1220–1228. doi: 10.1109/TBME.2015.2491270.
- Liu, Jiankun, Jin Oh Hahn & Ramakrishna Mukkamala. 2013. Error mechanisms of the oscillometric fixed-ratio blood pressure measurement method. *Annals of Biomedical Engineering* 41(3). 587–597Theory of the oscillometric maximum and the.
- Martonik, Andrew. 2014. How to use the heart rate monitor on the galaxy s5. https://www.androidcentral.com/how-use-heart-rate-monitor-galaxy-s5.
- Mauck, G. W., C. R. Smith, L. A. Geddes & J. D. Bourland. 1980. The Meaning of the Point of Maximum Oscillations in Cuff Pressure in the Indirect Measurement of Blood Pressure—Part II. *Journal of Biomechanical Engineering* 102(1). 28–33.
- Mukkamala, Ramakrishna & Jin Oh Hahn. 2018. Toward ubiquitous blood pressure monitoring via pulse transit time: predictions on maximum calibration period and acceptable error limits. *IEEE Transactions on Biomedical Engineering* 65(6). 1410–1420.
- Mukkamala, Ramakrishna, Jin Oh Hahn, Omer T. Inan, Lalit K. Mestha, Chang Sei Kim, Hakan Toreyin & Survi Kyal. 2015. Toward ubiquitous blood pressure monitoring via pulse transit time: theory and practice. *IEEE Transactions on Biomedical Engineering* 62(8). 1879–1901. doi:10.1109/TBME.2015.2441951.
- Muntner, Paul, Daichi Shimbo, Robert M. Carey, Jeanne B. Charleston, Trudy Gaillard, Sanjay Misra, Martin G. Myers, Gbenga Ogedegbe, Joseph E. Schwartz, Raymond R. Townsend, Elaine M. Urbina, Anthony J. Viera, William B. White & Jackson T. Wright. 2019. Measurement of Blood Pressure in Humans: A Scientific Statement From the American Heart Association. *Hypertension* 73(5). e35–e66.
- Ng, Kim-Gau & Carolyn F. Small. 1994. Survey of automated noninvasive blood pressure monitors. *Journal of Clinical Engineering* 19(6). 452–475.
- NIH. 2002. National high blood pressure education program/national heart, lung, and blood institute and american heart association working meeting on blood pressure measurement. https://www.nhlbi.nih.gov/files/docs/resources/heart/bpmeasu.pdf.

- Pickering, Thomas G, Daichi Shimbo & Donald Haas. 2006. Ambulatory blood-pressure monitoring. *The New England Journal of Medicine* 354(22). 2368–2374.
- Picone, Dean S., Martin G. Schultz, Petr Otahal, Svend Aakhus, Ahmed M. Al-Jumaily, J. Andrew Black, Willem J. Bos, John B. Chambers, Chen Huan Chen, Hao Min Cheng, Antoine Cremer, Justin E. Davies, Nathan Dwyer, Brian A. Gould, Alun D. Hughes, Peter S. Lacy, Esben Laugesen, Fuyou Liang, Roman Melamed, Sandy Muecke, Nobuyuki Ohte, Sho Okada, Stefano Omboni, Christian Ott, Xiaoqing Peng, Telmo Pereira, Giacomo Pucci, Ronak Rajani, Philip Roberts-Thomson, Niklas B. Rossen, Daisuke Sueta, Manish D. Sinha, Roland E. Schmieder, Harold Smulyan, Velandai K. Srikanth, Ralph Stewart, George A. Stouffer, Kenji Takazawa, Jiguang Wang, Berend E. Westerhof, Franz Weber, Thomas Weber, Bryan Williams, Hirotsugu Yamada, Eiichiro Yamamoto & James E. Sharman. 2017. Accuracy of Cuff-Measured Blood Pressure: Systematic Reviews and Meta-Analyses. *Journal of the American College of Cardiology* 70(5). 572–586.
- Pressman, G. L. & P. M. Newgard. 1963. a Transducer for the Continuous External Measurement of Arterial Blood. *IEEE Transactions on Bio-medical Electronics* 10(2). 73–81.
- Psaty, Bruce M., Nicholas L. Smith, David S. Siscovick, Thomas D. Koepsell, Noel S. Weiss, Susan R. Heckbert, Rozenn N. Lemaitre, Edward H. Wagner & Curt D. Furberg. 1998. Health outcomes associated with antihypertensive therapies used as first-line agents. *Survey of Anesthesiology* 1997(9). 739–745.
- Raamat, R., J. Talts, K. Jagomägi & E. Länsimies. 1999. Mathematical modelling of non-invasive oscillometric finger mean blood pressure measurement by maximum oscillation criterion. *Medical and Biological Engineering and Computing* 37(6). 784–788.
- Raamat, Rein, Jaak Talts, Kersti Jagomägi & Jana Kivastik. 2011. Errors of oscillometric blood pressure measurement as predicted by simulation. *Blood Pressure Monitoring* 16(5). 238–245.
- Ramsey, Maynard. 1979. Noninvasive automatic determination of mean arterial pressure. *Medical & Biological Engineering and Computing* 17(1). 11–18.
- Reisinger, Don. 2008. Apple's iphone x sales have been strong—but not record-breaking, analyst says. https://fortune.com/2018/01/23/apple-iphone-x-sales-2/.
- Rosner, Bernard & B Frank Polk. 1983. Predictive values of routine blood pressure measurements in screening for hypertension. *American Journal of Epidemiology* 117(4). 429–442.
- Seo, Joohyun, Sabino J. Pietrangelo, Hae Seung Lee & Charles G. Sodini. 2015. Noninvasive arterial blood pressure waveform monitoring using two- Element ultrasound system. *IEEE Transactions on Ultrasonics, Ferroelectrics, and Frequency Control* 62(4). 776–784.
- Shaltis, Phillip A., Andrew T. Reisner & H. Harry Asada. 2008. Cuffless blood pressure monitoring using hydrostatic pressure changes. *IEEE Transactions on Biomedical Engineering* 55(6). 1775–1777.

- by Statista. 2018. Share of iphone installed base worldwide model. of 2018. https://www.statista.com/statistics/755593/ as may iphone-model-device-market-share-worldwide/.
- Statista. 2019. Number of smartphone users worldwide from 2016 to 2021 (in billions). https://www.statista.com/statistics/330695/number-of-smartphone-users-worldwide/.
- Strauch, Berish & Wilson de Moura. 1990. Arterial system of the fingers. *Journal of Hand Surgery* 15(1), 148–154.
- Thijs, Lutgarde, Tine W. Hansen, Masahiro Kikuya, Kristina Björklund-Bodegård, Yan Lie, Eamon Dolan, Valérie Tikhonoff, Jitka Seidlerová, Tatiana Kuznetsova, Katarzyna Stolarz, Manuel Bianchi, Tom Richart, Edoardo Casiglia, Sofia Malyutina, Jan Filipovský, Kalina Kawecka-Jaszcz, Yuri Nikitini, Takayoshi Ohkuboc, Edgardo Sandoya, Jiguang Wang, Christian Torp-Pedersen, Lars Lind, Hans Ibsen, Yutaka Imai, Jan A. Staessen & Eoin O'Brienl. 2007. The International Database of Ambulatory blood pressure in relation to Cardiovascular Outcome (IDACO): Protocol and research perspectives. *Blood Pressure Monitoring* 12(4). 255–262.
- Ursino, Mauro & Cristina Cristalli. 1996. A mathematical study of some biomechanical factors affecting the oscillometric blood pressure measurement. *IEEE Transactions on Biomedical Engineering* 43(8). 761–778.
- Van Montfrans, Gert A. 2001. Oscillometric blood pressure measurement: Progress and problems. *Blood Pressure Monitoring* 6(6). 287–290.
- Vappou, J., J. Luo, K. Okajima, M. Di Tullio & E. E. Konofagou. 2011. Non-invasive measurement of local pulse pressure by pulse wave-based ultrasound manometry (PWUM). *Physiological Measurement* 32(10). 1653–1662.
- Weber, Michael A. 2015. Interpreting Blood Pressure in Young Adults. *Journal of the American College of Cardiology* 65(4). 336–338.
- Wesseling, Karel H., Jos J. Settels, Gerard M.A. Van Der Hoeven, Jannes A. Nijboer, Michelle W.T. Butijn & Joop C. Dorlas. 1985. Effects of peripheral vasoconstriction on the measurement of blood pressure in a finger. *Cardiovascular Research* 19(3). 139–145.
- Wu, Jin Chu. 2008. Statistical analysis of widths and heights of fingerprint images in terms of ages from segmentation data. https://www.nist.gov/sites/default/files/finger_size_age.pdf.
- Yano, Yuichiro, Jeremiah Stamler, Daniel B. Garside, Martha L. Daviglus, Stanley S. Franklin, Mercedes R. Carnethon, Kiang Liu, Philip Greenland & Donald M. Lloyd-Jones. 2015. Isolated systolic hypertension in young and middle-aged adults and 31-year risk for cardiovascular mortality: The Chicago heart association detection project in industry study. *Journal of the American College of Cardiology* 65(4). 327–335.